Phase 1 clinical study of an embryonic stem cell–derived retinal pigment epithelium patch in age-related macular degeneration

Lyndon da Cruz[1–4], Kate Fynes[1], Odysseas Georgiadis[1–3], Julie Kerby[5,6], Yvonne H. Luo[1–3], Ahmad Ahmado[1], Amanda Vernon[7], Julie T. Daniels[7], Britta Nommiste[1], Shazeen M Hasan[1], Sakina B Gooljar[1], Amanda-Jayne F. Carr[1], Anthony Vugler[1], Conor M. Ramsden[1,3], Magda Bictash[5], Mike Fenster[5] , Juliette Steer[5] , Tricia Harbinson[5] , Anna Wilbrey[5] , Adnan Tufail[2,3], Gang Feng[5], Mark Whitlock[5], Anthony G. Robson[2,3], Graham E. Holder[2,3], Mandeep S. Sagoo[2,3], Peter T. Loudon[5], Paul Whiting[5,8] & Peter J Coffey[1,2,9]

[1]The London Project to Cure Blindness, ORBIT, Institute of Ophthalmology, University College London (UCL), London, UK.
[2]NIHR Biomedical Research Centre at Moorfields Eye Hospital NHS Foundation Trust, UCL Institute of Ophthalmology, London, UK.
[3]Moorfields Eye Hospital NHS Foundation Trust, London, UK.
[4] Wellcome/EPSRC Centre for Interventional & Surgical Sciences (WEISS), Charles Bell House, London, UK.
[5]Pfizer, Granta Park, Cambridge, UK.
[6]Cell and Gene Therapy Catapult, London, UK.
[7]Cells for Sight, Transplantation & Research Program, UCL Institute of Ophthalmology, London, UK.
[8]UCL Institute of Neurology, Queen Square, London, UK.
[9]Center for Stem Cell Biology and Engineering, NRI, UC, Santa Barbara, CA, USA.

Corresponding Author:

L. da Cruz[1, 2, 3, 4] email: Lyndon.dacruz@Moorfields.nhs.uk

ABSTRACT

Age-related macular degeneration (AMD) remains a major cause of blindness, with dysfunction and loss of retinal pigment epithelium (RPE) central to disease progression. We engineered an RPE patch comprising a fully differentiated, human embryonic stem cell (hESC)–derived RPE monolayer on a coated, synthetic basement membrane. We delivered the patch, using a purpose-designed microsurgical tool, into the subretinal space of one eye in each of two patients with severe exudative AMD. Primary endpoints were incidence and severity of adverse events and proportion of subjects with improved best-corrected visual acuity of 15 letters or more. We report successful delivery and survival of the RPE patch by biomicroscopy and optical [AU: OK?] coherence tomography, and a visual acuity gain of 29 and 21 letters in the two patients, respectively, over 12 months. Only local immunosuppression was used long-term. We also present preclinical, surgical, cell safety and tumorigenicity studies leading to trial approval. This work supports the feasibility and safety of hESC-RPE patch transplantation as a regenerative strategy for AMD.

INTRODUCTION

Human ESCs represent a promising source for cellular replacement therapies owing to their availability, pluripotency, and unlimited self-renewal capacity. However, they also carry risks of neoplastic change, uncontrolled proliferation, and differentiation to inappropriate cell types[1, 2]. The eye is advantageous in investigating hESC-based cell therapy, as it is accessible and confined, and the transplanted cells can be monitored directly *in vivo*, with the possibility of being removed or destroyed if there is evidence of neoplastic change[3, 4]. Furthermore, long-term immunosuppression can be delivered locally.

Late AMD is characterized by irreversible cell loss, initially of RPE cells and subsequently of neuroretinal and choroidal cells[5], and thus may be amenable to hESC-based cell therapy[4]. The disease process includes damage to the RPE's specialized basement membrane, Bruch's membrane[5]. Currently, treatments exist only for the exudative or 'wet' form of AMD. These treatments rely on angiogenesis inhibitors [6] or indirect transplantation of an autologous RPE-Bruch's complex (retinal translocation surgery) [7].

However, the former treatment only suppresses the disease, requiring long-term repeat delivery, and the latter, although restoring the macular anatomy, does not prevent disease recurrence. It is possible that hESC-RPE patch may alter the natural history of the disease as the cells are zero years old, rather than the 60 plus years of the patients, and it does not contain predisposition to develop AMD that the host cells have already manifest, however, only further investigations will address this. There is no treatment for atrophic 'dry' AMD, which is characterized by RPE loss and progressive neuroretinal cellular dysfunction.

Suspensions of hESC-derived RPE (hESC-RPE) cells have been transplanted in human subjects with dry AMD and Stargardt's disease, but the extent of cell survival and restoration of vision remains ambiguous [8]. A recent, single-patient report described transplantation of an autologous induced pluripotent stem cell (iPSC)–derived RPE patch on its own secreted basement membrane[29]. The iPSC-RPE survived with maintenance, but no improvement, of visual acuity at 12 months. We developed a therapeutic, biocompatible hESC-RPE monolayer on a coated synthetic membrane, herein termed a 'patch', for transplantation in wet and early-stage dry AMD. The choice of membrane material and its preparation, including the human vitronectin coating, has not been described previously to our knowledge. In contrast to RPE suspensions, cells on the patch are delivered fully differentiated, polarized, and with the tight junction barrier formed, that is, in a form close to their native configuration. The synthetic membrane allows the patch to be handled easily and robustly. The main disadvantage of the patch is that it requires a purpose-built delivery tool and a more complicated surgery compared to cell suspensions, and the use of hESCs may require immunosuppression, unlike an autologous cell source. Our delivery tool (Supplementary figure 1) confers the benefit of protecting the patch within the tip, thereby minimizing cell loss, cell distribution within the eye, and physical damage to the RPE monolayer.

The clinical trial was designed as a phase 1, open-label, safety and feasibility study of implantation of a hESC-RPE patch in subjects with acute wet AMD and recent rapid vision decline. For safety reasons and to obtain an early efficacy signal, the initial clinical trial involved patients with severe wet AMD only, although we aim to study the RPE patch in early dry AMD as well. We reported three serious adverse events to the regulator. These were exposure of the suture of the fluocinolone implant used for immunosuppression, a retinal detachment, and worsening of diabetes following oral prednisolone. All three

incidents required readmission to the hospital, with the first two incidents requiring further surgery and the third being treated medically. The three incidents were treated successfully. Both patients achieved an improvement in vision of more than 15 letters, which was sustained for 12 months.

RESULTS

Engineering an RPE patch

Our protocol for manufacturing a clinical-grade RPE patch is summarized in **Figure 1**. RPE cells were differentiated from the SHEF-1.3 hESC line, which had been derived from the SHEF1 hESC line. We used a spontaneous differentiation method [9], an approach that has been described earlier by others and has been applied to primate [10] and human [11, 12] ESCs. Spontaneous differentiation limits the need for additional factors, thus complying with good manufacturing practice (GMP) guidelines, and with clear advantages over vector-driven methods in terms of safety and stability of the final RPE. Our differentiation protocol differs from another similar protocol [9] in that we used Essential 8 medium rather than human feeder cells during expansion and the early phase of differentiation to avoid exposure to another cell type and to fulfill GMP guidance. While several methods are used to produce hESC-RPE [10, 12, 13, 14], because of epigenetic variation from the earliest stages after derivation of hESCs, no method is universally effective [14, 15]. With our protocol, 20–30% of hESC colonies differentiated to RPE (data not shown), which is similar to that of other spontaneous methods [10, 12] but less efficient than some augmented methods [14-16].

Subsequent RPE characterization used immunocytochemistry, electron microscopy, pigment-epithelium-derived factor (PEDF) secretion profile testing, and a functional phagocytosis assay (**Fig. 2d**). During manufacturing, in-process testing, including *in situ* hybridization with a specific oligonucleotide probe for LIN28A mRNA[11], was undertaken to detect hESC impurity at the single-cell level. Differentiated RPE was discarded if any LIN28A-positive cells were detected. The hESC-RPE cells were seeded at confluence onto a human-vitronectin-coated polyester membrane. A 6 × 3 mm (17 mm^2) therapeutic element with ~100,000 cells (PF-05206388 in the regulatory documentation) was cut to size with a purpose-built punch and loaded into a sealed transport container (Fig. 1). Immediately prior to release for human transplantation, the cell layer was recharacterized as RPE according to a visual inspection release test encompassing cell dose, cell identity, and patch coverage checks.

Mouse teratoma and *in vitro* cell-spiking studies

The literature suggests that adult human RPE cells[17], terminally differentiated hESC-RPE[18], and spontaneously immortalized RPE cells[19] are non-proliferative cell types and appear to lack the potential to form teratomas. We tested tumorigenicity in NIH III nude mice. Cell suspensions were used as the mouse eye is too small to administer a patch. Two initial studies conducted with undifferentiated hESCs showed that teratomas could form. In these studies, cell suspensions were injected subretinally, intra-muscularly and subcutaneously, with mice followed for 26 weeks. Subsequently, we studied the tumorigenicity of hESC-RPE cells under good laboratory practice (GLP) conditions, including a positive control group injected with undifferentiated hESCs. Given our finding that undifferentiated hESCs formed teratomas, we conducted *in vitro* cell-spiking studies to examine whether hESCs survive the RPE manufacturing process and culture-seeding conditions.

In the first study, injection of 4.5–8.8 × 10^4 undifferentiated hESCs into the subretinal space of NIH III mice resulted in localized neoplastic formation in almost half the males injected (12/30) but in very few females (2/30). The tumors showed evidence of pluripotency and appeared to be composed of mesenchymal and epithelial lineages (data not shown).

In the second study of undifferentiated hESCs, neoplastic masses were observed in the injected eye of 12/15 female and 5/5 male mice after cell administration into the subretinal space. Teratomas were observed microscopically in the thigh of all female mice that received 3.6 × 10^4 or 8.23 × 10^5 undifferentiated hESCs in BD Matrigel by the intramuscular route, and in the left flank of 2/5 and 1/11 female mice that received 3.6 × 10^4 or 8.23 × 10^5 undifferentiated hESCs in BD Matrigel, respectively, by the subcutaneous route. Masses were composed of structures derived from all embryonic germ layers (data not shown).

In the third study, conducted with cells manufactured under GLP conditions, suspensions of hESC-RPE cells, or of undifferentiated hESCs as a positive tumorigenic control, were injected subretinally in NIH III mice. In a total of 80 mice injected with suspensions of hESC-RPE cells, no teratomas were detected (Fig 3B). Pigmented hESC-

RPE cells were observed lining the surface of the retina or lens in the injected eyes of some mice given 6.04 x 10^4 hESC-RPE cells (Fig.3 E1, E2 and E3 at 26 weeks (Fig.3E1). No premature death was associated with the injections.

In the same study, administration of undifferentiated hESCs was associated with ocular teratoma formation in four males and five females given 4.28 x 10^4 cells, all of which were prematurely euthanized (between days 46–62), and in a single male given 4.51 × 10^3 cells, which survived to the 26 week end point of the experiments (Fig 3C). In addition, mesenchymal tumors classified as “Not Otherwise Specified” were present in two males given 4.28 × 10^4 undifferentiated hESCs (Fig 3D) and perilenticular mesenchymal hyperplasia in animals of both sexes given 4.51 × 10^3 cells or 4.28 × 10^4 cells. All tumors were composed of human cells, as confirmed by immunohistochemistry using an anti-human mitochondrial marker (data not shown). Eyes injected with undifferentiated hESCs also exhibited an increase in the incidence and severity of non-proliferative changes, including lenticular degeneration, posterior synechiae of the iris, and retinal detachment (data not shown). Transplantation of either differentiated or undifferentiated hESCs did not affect body weight.

Given the tumor formation observed with undifferentiated hESCs, we aimed to determine whether hESC-RPE derived from SHEF-1.3 hESC contained any residual pluripotent cells or could support the survival of pluripotent cells, as this would constitute a teratoma risk. Immunostaining and flow cytometric analysis of cells expressing the pluripotency marker Tra-1-60 (Abcam 16288, Cambridge, UK) detected no undifferentiated hESCs in dissociated RPE foci prior to the expansion phase or at 6 to 8 weeks after seeding at the end of the expansion phase (Supplementary figure 2). We spiked undifferentiated hESCs into the RPE at 1, 10, 20 or 50% of total cells at the start of the expansion phase (see online methods). This did not affect the quality of the resulting 6-to-8-week-old cultures at the end of the expansion phase, which showed cobblestone morphology and pigmentation, and stained strongly for PMEL17 (an RPE marker that indicates the presence of premelanosomes). By 2 d post-spiking, viable Tra-1-60-positive cells were no longer detectable by flow cytometry (data not shown). This finding was supported by propidium iodide staining, which showed that ~96% of hESCs died when dissociated and seeded in the same manner as RPE prepared for expansion (Supplementary figure 3). The cells that survived in some experiments did not have hESC-

like morphology and failed to stain for Tra-1-60 or the proliferation marker Ki67, suggesting that they had differentiated or senesced (Supplementary figure 3 D&E).

Pig single-dose studies

Studies of surgical feasibility and safety of delivery of the RPE patch as well as studies of local and systemic biodistribution and toxicity were carried out in pigs. Human and pig eyes are similar in size, which allowed for administration of the full-size patch. Two studies were performed; the second used the same clinical surgical technique as in the human clinical trial. Biodistribution of hESC-RPE cells was evaluated in more than ten sites using qPCR detection of multiple human cell markers.

In the first pig study, patch delivery was successful in all 20 animals, as assessed by intraoperative observation of the patch under the neural retina and histological sections showing the patch in the subretinal space (figure 3 H & I). No retinal detachments were noted in any animal. We found surviving human cells by light microscopy at 2 h, 2 d, and 1, 2, 4, and 6 weeks after implantation (RPE patch: *n* = 12; control patch without cells: *n* = 8; figure 3 H-K). Human [AU: OK?] cell survival was demonstrated despite immunosuppression having been limited to the peri-operative period using oral prednisolone. Surviving cells remained pigmented (Fig. 3 J), expressed RPE-specific cell markers, showed no proliferation activity, and did not migrate away from the membrane (data not shown). **[AU: Clarify: 'Human' or 'Human or pig'?]** Pig photoreceptor survival above the patch was observed only in animals that received an RPE patch, as assessed by histology (Fig. 3H). The control membrane without cells did not pig photoreceptor survival (Fig. 3I). Microscopically, retinal architecture was intact in most animals receiving human cells. Macrophages were seen and appeared to have phagocytosed some transplanted RPE cells to form large pigmented cells (data not shown). Lymphocytic infiltrate was not observed except in 2 animals at 2 and 6 weeks. Animals that received the control membrane also had macrophage infiltrates but no lymphocytic response (data not shown). These results demonstrated that patch transplantation with hESC-RPE survival was surgically feasible without significant safety issues.

The second pig study differed from the first in that we used the purpose-built surgical tool, which has a protective cradle at the tip from which the patch is mechanically pushed out when the tip is in the subretinal space (Supplementary figure 1). The study was

undertaken under GLP conditions, a standardized set of requirements to ensure quality and systematic management of the experiment. In this case, it dictated standards for the operating and animal facilities and for the personnel who ran the trial, and defined the conditions and requirements for the keeping and monitoring of animals in the study, including the feeding regimen. Correct surgical delivery of ten RPE patches and ten coated membranes without RPE was achieved in 20 pigs as assessed by clinical examination and histology (Figure 3 F & G). Good cell cover was observed at the 6-week time point in the ten animals that received RPE cells (Fig. 3F). Retinal detachment and rupture of the lens capsule were observed in one male and one female implanted with the patch. There was no evidence of weight loss or early death in any animal. At 6 months after implantation, no hESC-RPE cells were detected at the implantation site or elsewhere in H&E sections of the ten eyes receiving the RPE patch. Anti-human TRA-1-85 immunostaining of the operated eye and optic nerve from these animals was also negative. Microscopic findings of chronic inflammation were seen restricted to the subretinal implantation site, at 6 months in the implanted (left) eye of all animals, and were consistent with the intraocular surgical implantation procedure. The microscopic findings included fibrosis, osseous metaplasia, and small numbers of macrophages and multinucleate giant cells (data not shown). Atrophy of the photoreceptor layer in overlying retina was also present (data not shown). Findings were of similar incidence and severity in both control and cell-treated animals. No positive amplification of any human-specific genes was observed in adrenal, bone marrow (rib and femur), brain, heart, kidneys, liver, lungs, lymph nodes, optic nerve, spleen, or thymus, which were evaluated by qPCR, indicating that the cells did not appear to migrate or survive away from the site of implantation. The second pig study confirmed the surgical feasibility and reliability of the delivery tool and the lack of systemic or local distribution of the hESC-RPE cells.

Clinical trial

Regulatory permission was granted for a phase I trial on the basis of the preclinical studies reported in this article, and published data on the hESC-RPE monolayer[9] (Clinical Trials.gov: NCT01691261). Permission was granted for ten patients, and we report the primary and secondary outcomes from the first two (Figs 4, 5, 6 and 7). In addition to safety, the trial investigated whether the synthetic membrane would facilitate mechanical delivery of the RPE monolayer, whether the transplanted cells could be sustained long-

term with local immunosuppression only, and whether early signals of potential efficacy were evident.

Using the surgical delivery tool, we placed one RPE patch in the subretinal space, under the fovea, in the affected eye of each patient. Correct placement was confirmed in both patients by stereo-biomicroscopy, fundus photography, and spectral domain optical coherence tomography (SD-OCT) (Figs. 4b1, b2 and 5b1, b2).

In patient 1, OCT and native-level autofluorescence immediately after surgery showed a 'double thickness' of RPE in one area nasal to the fovea, indicating overlap of native RPE and the patch (Figs. 4b, c, d). In all other areas of patient 1, and in all areas of patient 2, a single layer of RPE on OCT suggested there was no residual native RPE over the patch (figures 4b1 and 5b1). In both patients, hESC–RPE remained present over the full area of the patch at 12 months as evidenced by dark pigmented cells covering the patch, although unevenly, on fundus photography and a hyper-reflective monolayer on the patch seen by SD-OCT (figures 4a1,b1, 5a1, b1 and 6a and b). In both patients, the patches showed uneven autofluorescence (figures 4e3 and 5e3), which suggests functioning RPE phagocytosis [20, 21]. Also, visible in both patients were darker, pigmented areas continuous with the patch, which may represent RPE cell migration off the patch onto adjacent RPE-deficient areas. These areas spread from the patch edge outward over the first 6 months after surgery before stabilization (Fig. 6 a and b). The areas were contiguous with the patch RPE signal on OCT and were absent in areas where the native RPE layer persisted. There was no evidence of neoplastic transformation either on regular review of the fundus by an ocular oncologist or by serial ocular ultrasound.

In addition to RPE survival, we studied visual recovery. All measurements of visual acuity were made once before surgery and once at 12 months after surgery, and testing was always carried out by an independent qualified observer. The Early Treatment Diabetic Retinopathy Study (ETDRS) letter chart was used to define best corrected visual acuity (BCVA—vision with an optometrist-determined best glasses-corrected vision), which improved from 10 to 39 and from 8 to 29 letters, over 12 months in patients 1 and 2, respectively (Figs 7a and 7c). Microperimetry, a test of perception of microlocalized light stimuli, showed visual fixation at the center of the patch and vision over the patch in both patients (Figs. 4b1 and 5b1). Figures 4b1 and 5b1 show sample areas of visual sensitivity

localized totally within the patch. Over 12 months, reading speed improved from 1.7 to 82.8 and from 0 to 47.8 words/min in patients 1 and 2, respectively, by Minnesota MN Read (figs 7b and 7d), an improvement and final level not found in the Submacular Surgery Trial [22]. Pelli–Robson contrast sensitivity scores (Log) improved from 0.45 to 1.35 in patient 1, and 0 to 1.05 in patient 2, over 12 months. At each point that showed microperimetry sensitivity over hESC-RPE, we observed choroidal filling by angiography (Figs. 4e1, 4e2, 5e1 and 5e2); RPE-autofluorescence (Figs. 4e3 and 5e3; and presence of the ellipsoid layer (indicative of preserved photoreceptors) by SD-OCT (Figs. 4c1, 4c2, 5c1 and 5c2). We note that it was not possible to ascertain whether the ellipsoid zone was present pre-operatively, owing to the poor detail in the pre-operative OCT scans (Figs. 4a2 and 5a2). Rtx1 Adaptive optics camera images showed survival of cone photoreceptors in the areas corresponding to areas of sensitivity on microperimetry (Figures 4d1, 4d2, 5d1 and 5d2).

We reported three serious adverse events that were unrelated to the RPE patch. The first was exposure of the suture of the fluocinolone implant in patient 1, which required conjunctival revision surgery. The other two, both in patient 2, were a worsening of diabetes following oral prednisolone, which was treated medically, and a retinal detachment. The retinal detachment was an asymptomatic, infero-temporal, proliferative vitreoretinopathy (PVR)-associated traction retinal detachment under silicone, which did not extend past the inferior arcade and thus did not affect the implant. It was observed at the 8-week follow-up, with the retina having been completely attached at the 4-week check. It was treated with a single surgery with peeling of the PVR membranes, inferior retinectomy of the peripheral retina (180 degrees), and laser to the retinectomy edge. The silicone oil was retained. The retina was attached at the end of the surgery and has remained attached after subsequent surgery to remove the silicone oil. There was a residual epiretinal band over the posterior pole with some focal macular traction (figures 5b1 and 6b.), which was not treated.

Ocular pressures were never raised in either patient. No changes of concern were noted in the liver and renal function tests and by liver ultrasound in either patient. On full-field electro-retinography (ERG) recording, there was evidence of a mild but consistent reduction in photoreceptor function at 6 months in both patients with additional consequent Electro-oculography (EOG) reduction (in the operated eyes). The reduction in photoreceptor function persisted in patient 1 but recovered in patient 2 by 12 months.

Discussion

The results presented here provide an early indication of the safety and feasibility of manufacturing an hESC-RPE monolayer on a synthetic basement membrane and delivering the patch into the subretinal space as a potential treatment for AMD. Our data suggest early efficacy, stability, and safety of the RPE patch for up to 12 months in two patients with severe vision loss from very severe wet AMD.

hESC-RPE on a membrane shows optimized differentiation, polarization, viability, and maturation of the monolayer at the time of delivery that contrasts favorably with delivery of cell suspensions, where the cells are necessarily not in a monolayer and thereby not polarized or fully differentiated. Proper orientation is readily confirmed by the color difference between the white membrane and the pigmented RPE. Cells delivered in suspension may be lost due to reflux through the retinotomy, with potential vitreous seeding, and the cells undergo shear stress and damage when ejected through the delivery cannula[23]. Furthermore, cells in suspension are required to adhere to and form a monolayer on a damaged native Bruch's membrane, which leads to poorer cell survival and widespread apoptosis[24]. Previous work showed poor differentiation using suspensions and that RPE monolayers on membranes appear superior[25].

Therapeutic human RPE patch transplantation has been reported using a harvested autologous RPE–Bruch's membrane–choroid patch from the same eye [26, 27, 28] and an induced pluripotent stem cell (iPSC)-derived RPE patch[29]. The main advantages of our system over these were mechanical ease of handling due to the rigidity of the synthetic membrane. The tool we developed also allowed consistent patch delivery with a small localized retinal detachment over the macula, whereas with the intraoperative harvested autologous technique, half of the entire retina must be reflected to ensure consistent delivery without RPE damage[30, 31]. The availability of an off-the-shelf patch is especially advantageous and critical in cases of severe wet AMD with sudden vision loss, as described in this study. Treatment is required rapidly[32], and an autologous iPSC patch could not be prepared in a suitable time frame for transplantation. The main disadvantage of our technology is the need for immunosuppression, although for the two cases reported here we have demonstrated that only local immunosuppression is necessary for long-term hESC-RPE survival.

We present key preclinical safety and tumorigenicity studies that supported regulatory approval of our clinical study. The GLP study of tumorigenicity in NIH III mice showed that the hESC-RPE was not associated with tumor formation or other notable proliferative changes. Injected hESC-RPE cells survived for the full 26 weeks in some animals. Transplantation of undifferentiated hESCs under the same conditions was associated with teratoma formation as well as unclassified mesenchymal tumors, peri-lenticular mesenchymal hyperplasia, and an increase in the incidence and severity of degenerative changes in the treated eye (fig 3C and 3D).

Owing to tumor formation by undifferentiated hESCs, the major safety concern became the potential for survival and persistence of undifferentiated hESCs through the manufacturing process. In-process testing for undifferentiated cells is essential in the manufacture of any cell product from pluripotent cells for human transplantation. Spiking studies and single-cell labeling studies demonstrated no detectable undifferentiated cells in the final product. Even when we contaminated primary foci of hESC-RPE cells with up to 50% undifferentiated hESCs, no pluripotent hESC cells were present by the end of the expansion phase. Furthermore, hESCs were not viable when dissociated and seeded into RPE expansion conditions. Thus, we demonstrated that undifferentiated hESCs were not detectable at stage 4 of the production process, and that the RPE differentiation medium does not support the survival of hESCs.

Our preclinical studies in pigs investigated surgical feasibility, biodistribution, and toxicity. We showed consistent facilitated mechanical delivery of the RPE patch in all 20 pigs operated on in the GLP final study using our purpose-built tool. Implantation of the control membrane without cells led predictably to a foreign body reaction, but this was minimal when RPE cells covered the membrane. The presence of RPE was also associated with persistence of the native photoreceptor layer and less retinal atrophy than membrane alone in both pig and clinical studies (Figures 3H, 3I, 4c1, 4c2, 4d1, 5c1, 5c2 and 5d1).

A qPCR analysis of systemic biodistribution in pigs at 26 weeks after implantation of one clinical-sized graft (~100,000 hESC-RPE cells) showed no evidence that cells migrated or survived away from the site of administration. The lack of distribution of the

cells is consistent with previous studies on ocular administration of RPE cells [19]. This is also supported by our NIH III mouse study, in which teratomas from undifferentiated hESCs were found only in the eye, where the cells had been administered, and not in tissues distal to the site, suggesting that undifferentiated hESCs do not migrate or do not survive away from the site of implantation.

In the GLP pig study with no immunosuppression, no definitive hESC-RPE cells were identified at 26 weeks, whereas persistent hESC-RPE cells were found at 6 weeks in the earlier pig studies in which some animals were immunosuppressed perioperatively), and at 26 weeks in the NIH III mouse teratoma studies (immune-deficient animals). Histology of the implanted patch at 6 weeks from animals in the first pig study showed persistence of human RPE and support of normal retinal architecture relative to animals receiving the membrane alone (Fig 7H and I.). Microscopic findings consistent with a localized chronic inflammatory reaction around the polyester membrane were present in animals from both groups in the GLP pig study at 6 months, in the absence of any RPE cell cover. There was no difference in the incidence or severity of the inflammatory reaction in either group.

In the human clinical trial, the transplanted RPE patch survived, as demonstrated by a clear RPE signal on OCT for 12 months and the visible persistence of a pigmented cellular monolayer, although some of these cells may have been pigmented macrophages. There was evidence of early auto-fluorescence in both patients 1 and 2, suggesting that RPE phagocytosis has commenced [20, 21]. The retina over the patch was thinned in patient 1 but not in patient 2, which may reflect a difference in pre-operative disease or level of microtrauma from manipulation during surgery. It is possible that the decrease in central pigmentation in patient 1 represented cell loss from delayed rejection. Both patients retained features of normal architecture and visible areas of the ellipsoid zone. Furthermore, there was clear evidence of retinal function over the patch, as demonstrated by fixation microperimetry, which showed focal sensitivity, and increased visual acuity and reading speed, all of which were sustained or improved over the 12 months of follow-up. However, in the absence of a control, proving the improvement was due to the transplant is not possible. The improvement in reading exceeded that of similar cases in the submacular surgery trial [22]. Visual function remained variable across the transplanted area, with poor

visual function and thinning centrally in patient 1, which we feel may reflect intra-operative surgical trauma.

While histological evidence of hESC-RPE survival is not possible, the extensive number of structural and functional features discussed above support the conclusion that the hESC-RPE survived. Furthermore, the presence of transplanted hESC-RPE cells immediately adjacent to the neuroretina suggest that they are associated with retinal function over the patch. We did not intentionally remove the subretinal choroidal neo-vascular membrane, but cannot exclude that it was removed inadvertently. Therefore, the effect of the original choroidal neovascular membrane on function remains ambiguous. However, the co-localization of choroidal perfusion, survival of hESC-RPE, retinal sensitivity, and presence of photoreceptors strongly support the conclusion that the visual improvement and stability was associated with the transplanted RPE patch.

Retinal detachment was the most severe clinical complication seen. The GLP pig studies had two retinal detachments in 20 animals, which is similar to the rates reported for early human autologous transplantation and translocation surgeries[33, 34]. The retinal detachment in patient 2 of the clinical trial was likely a PVR-associated detachment that occurred between 4 and 8 weeks. It was treated with a single operation using standard techniques. The retinal detachment did not extend far enough to reach the patch. However, despite the delivery of RPE cells on a patch and in a protected delivery device, both of which minimize the shedding of RPE cells into the vitreous, we cannot be certain that no hESC-RPE cells were released nor that they did not contribute to the risk of developing PVR. The true surgical risk can be assessed accurately only with a larger series of patients.

In patient 1, there was an area of native RPE over the patch that was clearly delineated and separate from the large area over the patch where the native RPE was lost and only hESC-RPE was present (Figs 3 and 5). Notably, the patient fixated not over native RPE but over the RPE patch. Subjectively, patient 1 acknowledged that vision is improved relative to the pre-operative state and that she can see letters and read directly with the central vision; however, she described troublesome distortion, similar to that experienced by patients who have had previous retinal detachment or wet AMD. The

second patient described his vision as continuously improving but also being ‘dimmer’ than before the onset of the disease, which is consistent with his longer-standing disease at presentation and, likely, more damaged neuroretina.

Reporting these first two cases at 12 months is valuable because the functional improvement, robust imaging data, lack of major safety concerns, and demonstration of sufficiency of local immunosuppression represent steps in support of hESC-based regenerative therapy for AMD and other diseases of the eye. We show that differentiation of hESCs into a therapeutic cell with delivery, survival and rescue of vision in very severe disease is feasible. Although 12 months is sufficient to begin to describe cell survival and clinical outcomes, it is early in terms of safety monitoring, especially for late teratoma formation. The patients will be followed for a total of 5 years after surgery. These two early cases are also instructive as they show an encouraging outcome despite very advanced disease, which increases the complexity of surgery and involves more-damaged neuroretina. Additionally, there was no evidence of recurrence of the neovascular membrane and no need to administer angiogenesis inhibitors to either patient at 12 months, although with only two cases it is difficult to attribute this to the transplant.

The role of immune privilege in the subretinal space remains ambiguous, and the immunological effect of the surgery and patch transplant is unknown. Stability of the transplant was achieved with immunosuppression consisting of perioperative oral prednisolone and long-term intraocular steroid implants. For patient 2, who has type II diabetes, there was a period of poor blood sugar control with the need to add insulin, due to the systemic steroid use. Given the concerns about long-term systemic immunosuppression, a notable finding of this study is that the transplanted hESC-RPE cells survived at least 12 months with only local immunosuppression. Although long-term, local immunosuppression can be provided in the eye without systemic side effects, the possibility of long-term ocular morbidity remains. In our two patients, there was no associated intraocular pressure rise or need for pressure-reducing medication.

Stem-cell-based tissue transplantation is a potentially effective treatment strategy for neurodegenerative or other diseases with irreversible cell loss. Here we addressed challenges related to engineering, manufacturing and delivering a clinical-grade hESC-RPE patch, leading to stabilization and improvement of vision for at least 12 months in two

subjects with severe vision loss from AMD. These findings support further investigation of our approach as an alternative treatment strategy for AMD.

Competing interests

J.K., M.B., M.F., J.S., T.H., G.F., M.W., P.T.L., and P.W. were all employees of Pfizer during the period of this clinical trial. This study was sponsored by Pfizer Inc.

L. d C and P.J.C. are named on 2 patents lodged by University College London (UCL) Business. They are Patent Application No. PCT/GB2009/000917 (for the patch) and International Patent Application No. PCT/GB2011/051262 (for the surgical tool).

Author Contribution

L. d C*,‡., P.T.L., P.W., and P.J.C. designed all of the animal studies and clinical study, developed the methodology for these studies, completed pig surgery*, completed human surgery‡, collected the data, performed the analysis, and wrote the manuscript.

K.F., J.K., A. A.,** A.Ve., J.T.D., B.N., S.M.H., S.B.G., A-J.F.C., A.Vu.**, C.M. R., M.B., M.F., J.S., T.H., A.W. Developed, isolated and prepared the hESC – RPE and completed the engineering of the hESC-RPE patch; assisted design and assisted in completing the mouse and pig studies, completed mouse surgery**; collected the data, performed the analysis, and assisted in writing of the manuscript.

O.G., Y.H.L., A.A., A.T., G.F., M.W., A.G.R., G.E. H., M.S.S., Assisted in design of the clinical study, developed the methodology, collected the data, performed the analysis, and assisted in writing the manuscript.

Acknowledgments

We acknowledge H. Moore, Stem Cell Derivation Facility, Centre for Stem Cell Biology (CSCB), University of Sheffield for derivation of the original SHEF-1 hESC line. P. Keane and M. Cheetham for comments on the paper. We thank R. McKernan for support and input throughout the project.

L. d C. and P.J.C. received the following grants and donations and would like to acknowledge that they were used to fund the studies reported in this article:

Anonymous Donor, USA, Establishment of The London Project to Cure Blindness -.
Lincy Foundation, USA, The London Project To Cure Blindness: Funding Towards The Production Of A Cell Based Therapy For Late Stage Age-Related Macular Degeneration - P12761.
Macular Disease Society Studentship – Donation.
MRC, Stem Cell Based Treatment Strategy For Age-Related Macular Degeneration (AMD) - G1000730.
Pfizer Inc, The Development Plan For A Phase I/IIa Clinical Trial Implanting HESC Derived RPE for AMD - PF-05406388.
Moorfields Biomedical Research Centre, National Institute for Health Research (NIHR) - BRC2_011.
The Michael Uren Foundation R170010A

REFERENCES

1. Atala, A. Human embryonic stem cells: early hints on safety and efficacy. *Lancet*. **25**, 689-90 (2012).

2. Carr, A.J. *et al.* Development of human embryonic stem cell therapies for age-related macular degeneration. *Trends Neurosci*.**36**, 385-95 (2013).

3. Nazari, H. *et al.* Stem cell based therapies for age-related macular degeneration: The promises and the challenges. *Prog Retin Eye Res*. **48**, 1-39 (2015).

4. Bharti, K. *et al.* Developing cellular therapies for retinal degenerative diseases. *Invest Ophthalmol Vis Sci.* **55**, 1191-202 (2014).

5. Bhutto, I., Lutty, G. Understanding age-related macular degeneration (AMD): relationships between the photoreceptor/retinal pigment epithelium/Bruch's membrane/choriocapillaris complex. *Mol Aspects Med*. **33,** 295-317 (2012).

6. Rosenfeld, P.J. *et al*. Ranibizumab for neovascular age-related macular degeneration. *N Engl J Med.* **355**, 1419-1431 (2006).

570 7. Muthiah, M.N. *et al.* Adaptive optics imaging shows rescue of macula cone
571 photoreceptors. *Ophthalmology*. **121,** 430-431 (2014).
572
573 8. Schwartz, S.D. *et al.* Human embryonic stem cell-derived retinal pigment epithelium in
574 patients with age-related macular degeneration and Stargardt's macular dystrophy: follow-
575 up of two open-label phase 1/2 studies. *Lancet.* **385**, 509-16 (2015).
576
577 9. Vugler, A. *et al.* "Elucidating the phenomenon of HESC-derived RPE: anatomy of cell
578 genesis, expansion and retinal transplantation." *Experimental neurology* **214**, 347-361
579 (2008).
580
581 10. Haruta M (1), Sasai Y, Kawasaki H, Amemiya K, Ooto S, Kitada M, Suemori H,
582 Nakatsuji N, Ide C, Honda Y, Takahashi M. In vitro and in vivo characterization of pigment
583 epithelial cells differentiated from primate embryonic stem cells. *Invest Ophthalmol Vis Sci*.
584 Mar;**45**(3):1020-5(2004).
585
586 11. International Stem Cell, I., Adewumi, O. *et al.* Characterization of human embryonic
587 stem cell lines by the International Stem Cell Initiative. *Nat Biotechnol*, **25**, 803-816(2007).
588
589
590 12. Klimanskaya, I. *et al.* Derivation and comparative assessment of retinal
591 pigment epithelium from human embryonic stem cells using transcriptomics. *Cloning Stem*
592 *Cells* **6**, 217–245, (2004).
593
594 13. Idelson, M. *et al.* Directed differentiation of human embryonic stem cells into functional
595 retinal pigment epithelium cells *Cell Stem Cell* **5**(4):396-408 (2009).
596
597 14. Skottman H., Dilber, M.S., Hovatta, O. The derivation of clinical- grade human
598 embryonic stem cell lines. *FEBS Lett*. **580**, 2875–2878 (2006).
599
600 15. Allegrucci, C., et al. Restriction Landmark Genome Scanning identifies culture-induced
601 DNA methylation instability in the human embryonic stem cell epigenome. *Hum. Mol.*
602 *Genet*. May 15;**16**(10):1253-68. (2007).
603

16. Lund, R. D., *et al.* Human embryonic stem cell-derived cells rescue visual function in dystrophic RCS rats. *Cloning Stem Cells* **8(3):** 189-199 (2006).

17. Algvere, P. V., P. Gouras, and E. Dafgard Kopp. Long-term outcome of RPE allografts in non-immunosuppressed patients with AMD. *Eur J Ophthalmol*, **9**: 217-30 (1999).

18. Wang S, Lu B, Girman S, Holmes T, Bischoff N, Lund RD. Morphological and functional rescue in RCS rats after RPE cell line transplantation at a later stage of degeneration. Invest Ophthalmol Vis Sci. Jan;**49**(1):416-21 (2008).

19. Lu B, Malcuit C, Wang S, Girman S, Francis P, Lemieux L, Lanza R, Lund R. Long-term safety and function of RPE from human embryonic stem cells in preclinical models of macular degeneration. *Stem Cells*. Sep;**27**(9):2126-35 (2009).

20. Janet R. Sparrow and Tobias Duncker. Fundus Autofluorescence and RPE Lipofuscin in Age-Related Macular Degeneration. *J. Clin. Med.* **3**(4), 1302-1321; Review (2014).

21. The Atlas of Fundus Autofluorescence Imaging - edited by Frank G. Holz, Steffen Schmitz-Valckenberg, Richard F. Spaide, Alan C. Bird

22. Bressler, N.M. *et al.* Submacular Surgery Trials (SST) Research Group. Surgery for hemorrhagic choroidal neovascular lesions of age-related macular degeneration: ophthalmic findings: SST report no. 13. *Ophthalmology*. **111**, 1993-2006 (2004).

23. Mahetab H. Amer, Lisa J. White and Kevin M. Shakesheff. The effect of injection using narrow-bore needles on mammalian cells: administration and formulation considerations for cell therapies *Journal of Pharmacy and Pharmacology* **67**:640–650 (2015).

24. Tezel, T. et al. Reengineering of Aged Bruch's Membrane to Enhance Retinal Pigment Epithelium Repopulation *Invest Ophthalmol Vis Sci* **45**, 3337-3348 (2004)

25. Diniz, B. *et al*. Subretinal implantation of retinal pigment epithelial cells derived from human embryonic stem cells: improved survival when implanted as a monolayer. Invest Ophthalmol Vis Sci. **54**(7):5087-96 (2013).

26. Stanga P.E. *et al.* Retinal pigment epithelium translocation after choroidal neovascular membrane removal in age-related macular degeneration. *Ophthalmology* Aug;**109**(8):1492-8 (2002).

27. van Zeeburg E.J. *et al.* A free retinal pigment epithelium-choroid graft in patients with exudative age-related macular degeneration: results up to 7 years. *Am J Ophthalmol* Jan;**153**(1):120-7 (2012).

28. Chen F.K. *et al.* Long-term visual and microperimetry outcomes following autologous retinal pigment epithelium choroid graft for neovascular age-related macular degeneration. *Clin Exp Ophthalmol* Apr;**37**(3):275-85 (2009).

29. Mandai, M *et al.* Autologous Induced Stem-Cell-Derived Retinal Cells for Macular Degeneration. *N Engl J Med*. **16**;376(11):1038-1046 (2017).

30 van Romunde S.H.M. *et al.* Retinal Pigment Epithelium-Choroid Graft with a Peripheral Retinotomy For Exudative Age-Related Macular Degeneration: Long-Term Outcome. *Retina*. Nov 16 (2017).

31. Cereda M.G., Parolini B., Bellesini E., Pertile G. Surgery for CNV and autologous choroidal RPE patch transplantation: exposing the submacular space. *Graefes Arch Clin Exp Ophthalmol.* Jan;**248**(1):37-47 (2010).

32 Uppal G., Milliken A., Lee J., Acheson J., Hykin P., Tufail A., da Cruz L. New algorithm for assessing patient suitability for macular translocation surgery. *Clin Exp Ophthalmol.* Jul;**35**(5):448-57 (2007).

33 Pertile G., Claes C. Macular translocation with 360 degree retinotomy for management of age-related macular degeneration with subfoveal choroidal neovascularization. *Am J Ophthalmol*. Oct;**134**(4):560-5 (2002).

34 Chen F.K. *et al.* A comparison of macular translocation with patch graft in neovascular age-related macular degeneration. *Invest Ophthalmol Vis Sci.* Apr;**50**(4):1848-55 (2009).

Legends

Figure 1 Generation of hESC-derived RPE for the manufacture of an advanced therapeutic medicinal product to treat AMD.

This figure outlines the chronological process for manufacturing the RPE patch from SHEF-1.3 hESCs. The first four rows show the stages of differentiation; the coating on the plastic-ware for each step; the media used at each step; and the tests and checks performed at each step. The bottom row shows brightfield images illustrating each stage: **[AU: add column to image and label each row]** (i) hESC colonies expanded on recombinant human vitronectin (VTN-N). (ii) Spontaneously differentiated RPE cells appear as distinct pigmented foci.**[AU: line is offset; does that mean E8 medium is used at the beginning of SHEF-1.3 differentiation? Please clarify]** (iii) These foci are manually dissected, dissociated, and filtered to achieve a pure single-cell type RPE population, which is seeded onto plates, where expanding RPE cells establish their classic pigmented, cobblestone morphology. (iv) Fully differentiated RPE seeded at confluence. **[AU: add PET to text in figure as in v; deleted here]** (v) A therapeutic 'patch' consisting of the RPE monolayer immobilized on the vitronectin-coated PET membrane that has been cut from the transwell. (vi) Following release tests the advanced therapeutic medicinal product is supplied to the surgical team in a custom-manufactured single-use sterile container in saline, where it is viable for up to 8 h. PMEL17, premelanosome marker 17; ICC, immunocytochemistry; ISH, *in situ* hybridization; PET, polyethylene terephthalate; VIR test, visual inspection release test

Figure 2 Characterization of human hESC-derived RPE.

(**a**) Confocal bright-field immunofluorescent micrographs depicting staining for typical regional RPE markers as part of the characterization of the monolayer as RPE (each represents a single experiment with no repeats). Scale bars, 25 μm. Predominantly apical PEDF and basal BEST1 expression confirms polarity of these cells. PMEL17 expression confirms presence of premelanosomes, and ZO1 expression allows easy identification of tight junctions. Absence of Ki67 confirms that cells are not proliferating. Other characteristic RPE markers (CRALBP, MITF, OTX2), crucial for melanogenesis and visual cycle, are also present. Immunocytochemistry was performed once on SHEF-1.3-derived RPE cells. BEST1, bestrophin 1; CRALBP, cellular retinyladehyde-binding protein; DAPI, diamidino-2-phenylidole; MITF, microthalmia transcription factor; OTX2, orthodenticle homeobox 2; PEDF, pigment epithelium-derived factor; PMEL17, premelanosome protein 17; ZO1, zonula occludens 1.

(**b**) Quantification of PEDF secretion in spent culture medium during late expansion phase, analyzed using an ELISA assay. The classical RPE PEDF secretion asymptote is visible from around 3 weeks onwards. Each different colored box represents a separate batch of tested cells.

(**c**) Electron micrographs of RPE cells, illustrating the classical ultrastructure associated with normal RPE function including tight junctions (white arrows; i and iii), basal infoldings (black arrows; i and iv), apical microvilli (i–iii), and melanin granules (i–iii) revealing various stages of melanogenesis (ii; stage II/III, III melanosomes and stage IV mature melanosomes). Transmission electron microscopy was performed once on SHEF-1.3-derived RPE cells. N, nucleus; AmV, apical microvilli. Images represent a single experiment with no repeats.

(**d**) SHEF-1.3-derived RPE cells internalize photoreceptor outer segments (POS), demonstrating SHEF-1.3-derived RPE phagocytosis. The extent of phagocytosis was also examined after treatment of the SHEF-1.3 RPE with MERTK antibody (SHEF-1.3 RPE + blocker). Data shown are mean internalized POS ± s.e.m. (n = 3 biologically independent cell cultures in each group). Pre-incubation with MERTK antibody had a significant effect on the number of POS ingested by SHEF-1.3 RPE (P = 0.0000103075196107, two-tailed

730 Student's *t*-test, This was a single experiment with no replication. Below the graph,
731 confocal micrographs show the internalized POS with a green fluorescent marker (POS) in
732 SHEF-1.3-derived RPE and its relative absence in SHEF-1.3 RPE with MERTK antibody
733 (SHEF-1.3 RPE + blocker).
734
735 .
736

Figure 3 Preclinical mouse teratoma and pig transplantation studies.

NIH III immune-deficient mice preclinical teratoma studies.

(**a**) Normal non-injected eye of a mouse (H&E).

(**b**) 6-week-old animal injected with hESC-RPE (no teratomas or proliferation were observed in any animals from this group). Section taken 26 weeks after injection (H&E).

(**c**) An example of teratoma formation in an animal injected with undifferentiated hESC. Section taken following euthanization of the animal prior to 26 weeks (H&E).

(**d**) An example of a mesenchymal tumor NOS in an animal injected with undifferentiated hESC. Section taken at termination of the animal prior to 26 weeks (H&E).

(**e**, **i**) 6-week-old animal injected with hESC-RPE showing persistence of layers of pigmented cells at week 26. (**e**, **ii**) 6-week-old animal injected with hESC-RPE and examined with anti-human mitochondria IHC. Immunoreactivity for human mitochondria seen as a brown chromophore (black arrows), demonstrating that the cells represent implanted-hESC-derived RPE. (**e**, **iii**) 6-week-old animal injected with hESC-RPE and examined with an isotype control relative to section in **e**, **ii** with no positive staining (black arrows) using the same chromophore as in **e**, **ii**.

(**f**,**g**) *In vivo*, color fundus photographs of pig eyes from the GLP pig study taken 6 weeks after transplantation surgery. (**f**) The picture shows an eye that has been implanted with a 'patch' consisting of an hESC-derived RPE monolayer on a human-vitronectin coated polyester membrane. The patch is seen as a consistent and evenly pigmented cellular covering over the entire area. (**g**) Uncoated patch with no cells, which has been implanted as a control.

(**h**) Cresyl violet stain of pig retina at 6 weeks post-transplantation with a patch of RPE implanted into the subretinal space. INL, inner nuclear layer; ONL, outer nuclear layer.

(**i**) Cresyl violet stain of pig retina at 6 weeks post-transplantation with a patch without cells implanted into the subretinal space. GCL, ganglion cell layer; INL, inner nuclear layer. Note the absence of the ONL.

(**j**) Unstained pig retina 6 weeks post-transplantation with a patch of RPE cells which are pigmented (arrows highlight the position of the polyester membrane).

(**k**) Serial section from the same eye stained with anti-human TRA-1-85 indicates that the cells are human in origin (arrows highlight the position of the polyester membrane).

Figure 4. Case 1: Pre- and post-operative imaging of the cell patch with structural and functional outcomes at 12 months following surgery.

(**a**, **i**) Pre-operative color fundus photograph demonstrating the extensive sub-RPE and submacular hemorrhage extending under the fovea secondary to wet AMD. (**a**, **ii**) Spectral domain OCT (Spectralis, Heidelberg) showing pre-operative section with inset showing the position of the slice. (**b**, **i**) 12 months' postoperative color fundus photograph showing the patch covered with pigmented cells throughout. The test also shows microperimetry results with two areas of demonstrated sensitivity (Nidek microperimetry) labeled x and y. The circles represent the extent of the visual stimulus demonstrating that it falls completely within the transplanted area. Inset § shows a magnified detail of the patch area with the levels of sensitivity shown by microperimetry in decibels. Inset * shows a close up of the fixation with the Nidek microperimeter fixation outcome superimposed. (**b**, **ii**) Spectral domain OCT (Spectralis, Heidelberg) showing post-operative section with inset showing the position of the slice. The patch is shown in position with thinned retina over the area of the patch but an intact ellipsoid layer. (**c**, **i**,**ii**) Spectral domain OCT sections through x and y, respectively. The area on the section corresponding to x and y is indicated with a bar. The long red arrow in **c**, **i** and **c**, **ii** indicates the ellipsoid layer. The thin and bold green arrows in **c**, **i** and **c**, **ii** indicate the synthetic membrane and the hESC-RPE, respectively. (**d**, **i**) Images from the Rtx1 AO fundus camera. (Inset) Color fundus photo with superimposed area of AO imaging. The dotted yellow circle corresponds to the area of positive microperimetry sensitivity marked x throughout this figure. (**d**, **i**) Magnified image of the area indicated by the dotted yellow line in **g**, **i** showing bright dots corresponding to cone photoreceptors based on their size, inter-photoreceptor distance and organization (blue arrows). (**d**, **ii**) AO image taken from a normal patient at the same point of the retina as in **g**, **ii** for comparison. (**e**, **i**) Early-phase fundus fluorescein angiogram (FFA) showing early choroidal perfusion in the area of the patch and specifically the two points of demonstrated sensitivity x and y. The dark areas over the transplanted patch, at the nasal end of the patch and the superior border, represent areas of native RPE over and under the patch, masking emission rather than absent choroidal perfusion. (**e**, **ii**) Late-phase FFA confirming choroidal perfusion and no leakage under the patch. (**e**, **iii**) SLO autofluorescence over the patch, including in areas x and y, showing dim but visible autofluorescence.

Figure 5 Case 2: Pre- and post-operative imaging of the cell patch with structural and functional outcomes at 12 months after surgery.

(**a**, **i**) Preoperative color fundus photograph of the extensive sub-RPE and submacular hemorrhage extending under the fovea, secondary to wet AMD. (**a**, **ii**) Spectral domain OCT (Spectralis, Heidelberg) showing pre-operative section with inset showing the position of the slice. (**b**, **i**) 12 months post-operative color fundus photograph showing the patch covered with pigmented cells throughout. There is extensive epiretinal fibrosis associated with the extent of the disease and a retinal detachment that had been successfully reattached. The test also shows microperimetry (Nidek microperimetry) results with two areas of demonstrated sensitivity labeled x and y. Inset § shows a magnified detail of the patch area with the levels of sensitivity shown by microperimetry in decibels. Inset * shows a close-up of the fixation with the Nidek microperimeter fixation outcome superimposed. The circles represent the extent of the visual stimulus demonstrating that it falls completely within the transplant area. (**b**, **ii**) Spectral domain OCT (Spectralis, Heidelberg) showing post-operative section with inset showing the position of the slice. (**c**, **i**,**ii**) Spectral Domain OCT cuts through area x and y, respectively, as indicated. The detail shows the Spectral Domain OCT sections through x and y, respectively. The area on the section corresponding to x and y is indicated with a bar representing the area. The long red arrows indicate the ellipsoid layer. The thin and bold green arrows indicate the synthetic membrane and the hESC-RPE respectively. (**d**, **i**) Images from the Rtx AO fundus camera. Inset - color fundus photo with superimposed area of AO imaging. The magnified image of the area indicated shows bright dots corresponding to cone photoreceptors based on their size, inter-photoreceptor distance and organization. (**d**, **ii**) An Rtx AO fundus camera image taken from a normal patient at the same point of the retina as in **d**, **i** for comparison. (**e**, **i**) An early phase Fundus fluorescein angiogram (FFA) showing early choroidal perfusion in the area of the patch and particularly the two points of demonstrated sensitivity x and y. The dark areas temporal and superior to the transplanted patch likely represent areas of choriocapillaris loss associated with the primary pathology and surgery. (**e**, **ii**) Late phase FFA confirming choroidal perfusion and no leakage under the patch. (**e**, **iii**) SLO autofluorescence image over the patch including areas x and y demonstrating autofluorescence over parts of the patch.

Figure 6.

a. A sequence of colour photographs of the transplanted patch in case 1 at 4, 24, and 52 weeks. The sequence shows the centrifugal expansion of the pigmented areas around the patch and the stability of pigmented areas on the patch. It also shows the regression of the host RPE on the patch, with the original margin indicated by the dotted line. b. A sequence of colour photographs of the transplanted patch in case 2 at 4, 24, and 52 weeks. The sequence shows the centrifugal expansion of the pigmented areas around the patch and relatively stable areas of pigmentation on the patch. The expansion of pigmented areas in both 6a and b stabilized by week 24.

Figure 7.

a. Best Corrected Visual Acuity (BCVA) over 12 months for patient 1. b Reading speed over 12 months for patient 1. c. BCVA over 12 months for patient 2. d. Reading speed over 12 months for patient 2.

Online Methods.

Ethics statement

All animal (mouse and pig) procedures were conducted in accordance with the provisions of the United Kingdom Animals Scientific Procedures Act (ASPA) 1986. The animal experimentation under the ASPA is overseen by the Home Office, UK government, in England.

The mouse teratoma studies were carried out by the Independent Contract Research (CRO) Organization Huntington Life Sciences (HLS), now Envigo (Alconbury/Huntingdon, Cambridgeshire, UK). (HLS Animal Project - Licence number PCD 70/8702).

The pig surgery was carried out under GLP conditions at the Northwick Park animal experimental surgery facility (Northwick Park and St Mark's Hospital, Harrow, Middlesex, UK). Pigs were cared for in an independent GLP registered facility including throughout the 6-month's follow-up period. The animal reporting including organ sampling was carried out independently by HLS.

Clinical trial

Pfizer Inc. sponsored and was the sole funding source of the clinical trial. Two subjects out of a planned 10 were enrolled before Pfizer suspended funding for strategic commercial reasons unrelated to this trial. The cells for transplantation were prepared to the state of confluent RPE at Roslin Cells Ltd (Edinburgh, United Kingdom,) before transport to London. The preparation and cutting of the patch was completed at Cells for Sight (Institute of Ophthalmology, Bath St, London, UK).

Approval was granted from the U.K. Medicines and Health Products Regulatory Authority (MHRA), the Gene Therapy Advisory Committee (GTAC), the Moorfields Research Governance Committee and the London - West London & GTAC Research Ethics Committee. The study complied with Good Clinical Practice guidelines according to the European Clinical Trials Directive (Directive 2001 EU/20/EC), the Declaration of Helsinki and has an independent External Data Monitoring Committee (E-DMC). The data monitoring committee had three representatives who were retinal surgeons withtwo having

specialty expertise in ocular oncology and the third in ocular immunology. Informed consent was obtained from each patient. The study compliance with protocol was reviewed regularly, and none of the recorded protocol deviations had an impact on subject safety or study integrity

Reporting Summary

The *Nature Biotechnology* Reporting Summary has been completed and submitted with this article

Statistics

The only statistical analysis reported was for the phagocytosis study (Figure 2d). Data shown are mean ± s.e.m., $n = 3$ biologically independent cell cultures in each group. As the n is less than 10, individual data points are indicated. Analysis was by two-tailed Student's *t*-test with $P = 0.0000103075196107$. This was a single experiment with no replication.

Preparation of hESC-RPE (GMP conditions and facility).

The original cell source, the SHEF1 hESC (NIBSC - UK Stem Cell Bank - http://www.nibsc.org/ukstemcellbank) line was expanded according to GMP guidelines at the Stem Cell Derivation Facility, Centre for Stem Cell Biology (CSCB), University of Sheffield35. The SHEF 1 and 1.3 cell lines were authenticated by A Short-Term Repeat Analysis fingerprint, which was performed by University of Wisconsin Hospital and Clinics. The analysis showed an identical STR genotype profile across 8 human STR loci for both SHEF-1 and SHEF-1.3. The SHEF-1.3 cell line was derived from the expanded SHEF1 hESC cells under the same GMP conditions at the same facility. The passage and expansion of SHEF-1.3 hESCs was carried out in recombinant human vitronectin (VTN-N) (Life technologies)–coated culture vessels. Medium was removed from cultures and hESCs were washed with PBS-/-, incubated with EDTA (Sigma) until the cell colonies begin to detach. Cells were resuspended in Essential 8 (E8) medium (Life Technologies) and seeded onto VTN-N-coated culture vessels. hESC were replenished with E8 medium daily, and passaged every 3–4 d depending on visual observations of colony morphology and size.

hESC differentiation to RPE was carried out in flasks coated with plasma-derived vitronectin (Amsbio). Sets underwent regular media replenishment with E8 medium for up

to 14 d until hESC colonies were approximately 80 to 100% confluent and then transitioned to TLP medium consisting of 389ml of Knockout DMEM, 1 ml of 2-Mercaptoethanol, 5ml of NEAA, 100 ml of Knockout serum and 5 ml of L-glutamine per 500 mL. (Invitrogen – LifeTechnologies (Thermo Fisher Scientific). Cells were maintained on a twice-weekly media replenishment regimen. RPE cells appear in culture as distinct pigmented foci, visible to the naked eye, which continue to expand in diameter and can be maintained in this culture system for up to 22 weeks.

RPE foci were manually isolated using sterile microblades (Interfocus) and collected in TLP medium. Pooled foci were washed with PBS-/- and incubated at 37 ± 2 °C with Accutase (Sigma) until a cell suspension is observed. The suspension was then passed through a 70µm cell strainer (Corning), washed in TLP medium and counted. The cells were plated on CELLstart- coated (Life Technologies) 48-well plates at $4.8x10^4$ cells/well. Cells were maintained on a twice-weekly media replenishment regimen of TLP medium until they formed a confluent, pigmented cell sheet with cobblestone morphology, generally for a minimum of 5 weeks.

To ensure safety and purity of the RPE, it was essential to exclude the possibility of undifferentiated hESCs being administered to a patient. In situ hybridization was used to assess hESC impurity. Samples of differentiated cells were prepared as a monolayer on microscope slides. Specific oligo probes against LIN28A mRNA were used to evaluate the presence of hESC in the RPE population. LIN28A stained cells were identified using a nuclear stain. If any LIN28A positive cells were detected, the RPE batch would be rejected. Differentiated RPE were further assessed using immunocytochemistry against the melanosome-specific protein PMEL17 (Dako), an RPE cellular marker. PMEL17 positively stained cells were counted and expressed as a percentage of total cells. Upon testing of cells on representative cell patches, the RPE purity ranged from 99.8 to 100% on positive staining of PMEL17 and no LIN28A positive cells were detected.

RPE cells were assessed using a light microscope for pigmentation, cobblestone morphology, health and signs of contamination and processed further only if they passed this visual check. Media was removed, cells were washed with PBS-/-, and incubated at 37+/-2ºC with Accutase for 1–2 h until a cell suspension was observed. The suspension was passed through a 70µm cell strainer, washed in TLP medium and then counted. Cells

were subsequently seeded ($1.16x10^5$ cells/well) into custom manufactured transwells, with polyester membranes coated in plasma-derived human vitronectin. The membrane was 10µm thick polyethylene terephthalate (PET), with a 0.4µm pore size at a density of $1x10^8$ pores/cm^2 (Sterlitech, Kent, Washington, USA). TLP medium was added to the outer well containing the insert, and the plate then incubated at 37±2°C. The RPE cells were maintained with twice weekly TLP media replenishment until required for drug product manufacture.

On the day of surgery, the transwell was removed from the culture plate and placed directly onto the cutting device. The patch is cut from the membrane and is then placed into the storage solution (0.9% sodium chloride) within the storage container that is then sealed. (Figure 1a.) The patch is assessed visually through the clear lid of the storage container for integrity, pigmented cell coverage and viability. The patch was transported out of the GMP facility and transferred to the operating theatre.

Patch cell count.

The theoretical cell count on each patch was calculated using an observed cell diameter of 14um and this gives approximately 100,000 cells per patch. To complement this, two patches from preclinical production batches had the cells dissociated and counted and gave counts of 110,000 and 120,000 cells total (i.e. a cell diameter of approximately 12-13um). The theoretical cell count of 100,000 was within the confidence intervals from these two counts, and so was selected.

Immunocytochemistry.

Immunostaining was performed as described previously[16]. Briefly, cells were fixed in cold 4% paraformaldehyde (PFA) in 0.1M phosphate buffer and then blocked and incubated with an appropriate combination of the following primary antibodies: TRA-1-60 (Life Technologies); Ki67 (VectorLabs); CRALBP (Thermo Scientific); PMEL17 (Dako); MERTK (Abcam); ZO-1 (Life Technologies); OTX2 (Millipore); Bestrophin (Millipore) and PEDF (Millipore). They were then incubated in the appropriate secondary antibodies including AlexaFluor 647 conjugated donkey anti-mouse Ig-G (Life Technologies), 594 conjugated donkey anti-rabbit Ig-G (Life Technologies) and Dylight 488 conjugated donkey anti-mouse Ig-M (Startech). Nuclei were stained using Hoechst 33342 (Life Technologies).

Transmission electron microscopy (TEM) RPE cells immobilized on a membrane were fixed in Karnovsky's fixative and prepared for TEM as described previously[16].

PEDF assay on spent media was completed using a developmental ELISA (Meso Scale Discovery Platform S600, Mesoscale, USA) according to manufacturer's instructions**.**

Phagocytosis assay method

This was based on a previously described method [36]. Purification of photoreceptor outer segments (POS) was performed as described previously [37]. The POS were labeled as described previously[38]. The labeled POS were seeded onto hESC-RPE monolayer patches grown on plasma-derived human vitronectin at 1 x 10^7 POS/ml. In one condition the cells were pre-incubated with 1:50 anti MERTK antibody (ab52968, Abcam) to block phagocytosis for one hour. The cells were incubated at 37°C in 5% CO_2 for 6 hours. The samples were fixed and stained as described previously[38]. To quantify phagocytosis, 3 distinct areas per patch of hESC-RPE or hESC-RPE with blocker (MERTK antibody) (n=3) were imaged blind on the Zeiss 710 confocal. The total number of internalized fluorescent POS were counted in a 135µm x 135µm area, using the orthogonal view function.

Preclinical animal safety studies

Mouse teratoma studies.

The cells tested were undifferentiated SHEF-1.3 pluripotent hESCs (hereafter 'hESCs'), and SHEF-1.3 hESC-derived RPE ('hESC-RPE'). The cells were grown at a Pfizer facility before transfer to HLS. They were injected into the eyes of NIH III Immune-Deficient Mice (strain Crl:NIH-*Lyst* ^{bg}*Foxn1* ^{nu}*Btk* ^{xid}, 6-7 weeks old; Charles River, UK) at HLS. The injections were carried out by Antony Vugler & Ahmed Ahmadoo from University College London (UCL). Histological and pathological analyses were carried out by HLS, who provided a report on the study.

The second study was completed as there were fewer tumors in female animals in the first study. It was concluded that this was most likely linked to a decline in cell suspension quality for dosing of the females, rather than an actual sex difference. The second study, focused on female animals. In addition, we studied the relative rate of teratoma formation

following subretinal, subcutaneous (SC) or IM injection of undifferentiated hESCs in female NIH-III mice. In the second study five males were also dosed with undifferentiated hESCs subretinally.

In the third study, under GLP conditions, NIH III mice were administered suspensions of hESC-RPE cells or suspensions of undifferentiated hESCs as a positive tumorigenic control, with all injections being delivered subretinal. Other controls carried out in all the mouse teratoma studies are listed in the tables below. Animals were followed for up to 26 weeks, allowing for the assessment of tumors associated with the administration of the test cells, prior to the animals having an excessive burden of spontaneous tumors. The numbers of animals injected, the site and sex are listed in the following table.

Mouse teratoma studies

First study: 2-Month Pilot Study of the Teratoma Formation Potential of hESCs in NIH III Immune-Deficient Mice

Test condition	****Injected Number / sex animals***
1. Untreated Control	5/sex (10 total)
2. DMEM Control – Subretinal	5/sex (10 total)
3. hESCs at 45,000 M/44,000 F cells – Subretinal	15/sex (30 total)
4. hESCs at 88,000 M/68,000 F cells – Subretinal	15/sex (30 total)
5. Vehicle – IM	5/sex (10 total)
6. hESCs at 88,000 M / 68,000 F cells – IM	5/sex (10 total)

Second Study: 2-Month Pilot Study of the Teratoma Formation Potential of SHEF1-Cells in Female NIH III Immune-Deficient Mice

Test condition	****Injected Number / sex animals***
1. DMEM – Subretinal	5F (5 total)
2. hESCs at 35,600 cells – Subretinal	5/M (20 total)
	15/F
3. Matrigel – IM	5 F (5 total)
4. HESCS at 35,500 cells – IM	10F (10 total)
5. hESCs at 822,500 cells – IM	10F (10 total)
6. Matrigel – SC	5F (5 total)
7. hESCs at 35,500 cells – SC	8F (8 total)
8. hESCs at 822,500 cells – SC	12F (12 total)

Third Study (GLP conditions) Teratoma Formation Potential of hESC-RPE in NIH III Immune Deficient Mice for 26 Weeks Following Intraocular Dosing

Test condition	*Injected Number / sex animals*		
1. KO DMEM Control		10/sex	(20 total)
2. mTeSR™ Control		10/sex	(20 Total)
3. hESC-RPE at 5340 cells* in KO DMEM	20/sex	(40 Total)	
4. hESC-RPE at 60,400 cells* in KO DMEM	20/sex	(40 Total)	
5. hESCs at 4510 cells§ in mTeSR		19 M/20 F	(29 Total)
6. hESCs at 42,800 cells§ in mTeSR		20 M/19 F	(29 Total)

DMEM = Dulbecco's Modified Eagle Medium; KO DMEM = Knockout DMEM;
IM = Intramuscular; SC = Subcutaneous. M = Male; F = Female;
RPE = Retinal Pigment Epithelium;
§ Represents the average number of cells administered to the group.

Necropsy and histology.

At the end of the study animals were subject to a detailed necropsy and macroscopic examinations were performed on all treated and control animals. The following tissues were processed for histological examination: abnormal masses, epididymides, eyes, heart, kidneys, liver, lymph nodes (mesenteric, submandibular), optic nerves, ovaries, spleen, sternum with bone marrow, testes. Tissues and organs were collected and fixed in 10% neutral buffer except the eyes and optic nerves which were fixed in Davidson's fluid. Following histological processing and review any teratomas or abnormal masses were subject to immunohistochemistry (IHC) (anti-human mitochondrial marker staining), using a validated method to confirm whether these were of human or mouse origin.

Pig transplantation feasibility studies.

The analysis of the biodistribution data in pig tissues (looking for the evidence of human cells in different organs) was done using qPCR by the independent CRO Aros (Aarhus, Denmark) with reports provided.

Surgical safety, successful delivery of the RPE patch, local and systemic biodistribution and toxicology were examined in these studies. The pig was selected since the size of the pig eye allowed for the administration of the intended full-size patch and would allow the study of surgical feasibility, biocompatibility and biodistribution. All pig studies described were performed by the same surgeon who operated in the two cases described in the initial clinical trial. In the second pig study the same clinical surgical technique was used as in the human trial.

First pig study.

In this study, SHEF1-derived RPE cells were seeded onto a BD Matrigel (BD Biosciences, Erembodegem, Belgium)-coated polyester membrane and manually implanted as a 1x3 mm membrane into the subretinal space of pig eyes via 20G pars plana vitrectomy, bleb detachment with retinotomy followed by air tamponade. Twenty animals underwent surgery and 12 of these received *hESC-derived-RPE* cells on the membrane, 2 at each time point, with the remainder receiving a membrane without cells, 1 at each time point except 6 weeks where there were 3 animals. Six of the animals received immunosuppression with oral cyclosporine (650 mg for up to 2 weeks following surgery). Animals were observed, euthanized and enucleated at 2 hours, 2 d, 1, 2, 4, and 6 weeks. Eyes were examined by light and electron microscopy.

Second pig study.

Safety/Biodistribution Study of therapeutic patch in Pigs for 26 Weeks Following Surgical (Intraocular), subretinal Implantation

1. Control (vitronectin coated polyester membrane only)	5/sex (Total 10)
2. PF-05206388 1 graft (100,000 cells plus vitronectin coated polyester membrane)	5/sex (Total 10)

Toxicity.

The feasibility of the surgical procedure and the general safety of PF-05206388 was assessed in studies performed in the Large White/Landrace hybrid pigs (in all cases).

In the GLP pig study, a group of 5 male and 5 female pigs were administered a patch at a dose of 1 graft in the left eye (approximately 100,000 SHEF-1.3 derived RPE cells on a vitronectin coated polyester membrane) and observed for 26 weeks (6 months). A similarly constituted control group of 5 male and 5 female animals received the vitronectin coated polyester membrane only. The membrane with or without cells was placed into the subretinal space in all 20 pigs using the same tool and surgical technique as in the clinical trial. Animals received Prednisolone (1 mg/kg) orally 7 d before surgery, which continued for 14 d post operatively, intravitreal 4 mg Triamcinolone Acetonide (TCA) during the surgery, Sub tenon TCA 40mg at the end of surgery, and Carprofen (4 mg/kg) was given orally postoperative on day 2 of the study. Eye drops of 0.1% dexamethasone, 0.5%

hypromellose and 0.35% neomycin were administered to all the pigs 4 times per day for 17 d post-surgery.

Systemic distribution of cells.

The distribution of the hESC-RPE cells was evaluated as part of the pivotal 26-week toxicity study in pigs. The biodistribution was evaluated using qPCR techniques and the human cell markers huGAPD, huPEDF, HSSRY, huPOU5F1, and huOTX1/2 and the pig marker, pigACTB. A total of 60 samples from each animal (5/sex/group) that included the following: adrenal, bone marrow (rib and femur), brain (7 sections), heart (5 sections), kidneys (5 sections), liver (6 sections), lungs (5 sections), lymph nodes (4 nodes, total 8 sections), optic nerve (left and right, proximal and distal to eye), spleen (5 sections), thymus (3 sections) were evaluated. To avoid a high number of false positives, positives in at least 2 individual human markers in the same sample were required. There were no animals that received the matrix only that had an increase in amplifying human transcripts.

Cell spiking studies.

The effect of deliberately spiking hESCs into RPE was assessed. Different proportions (0, 1, 10, 20, 50 or 100%) of hESCs were mixed with dissociated RPE foci (P0 cells), seeded into 96 well plates at 38,000 cells/cm^2 and cultured for 6 weeks (P1 cells) using standard RPE culture conditions. Feeder-free hESC were used for spiking to eliminate counting inaccuracies due to the presence of fibroblast feeder cells. Plates were fixed and stained for TRA-1-60 or PMEL17 and the corresponding no primary antibody controls (n=4 plates, 1 well/plate stained with each antibody/control). A single cell suspension of hESCs was also seeded onto Matrigel in mTeSR1 media with ROCK inhibitor 2 d before fixing as a positive control for TRA-1-60 staining.

Flow cytometry.

Cells were washed with PBS and treated with Accutase to produce a single cell suspension, before pelleting and resuspended in 3% BSA/PBS to 1 million/ml. 100,000 cells per sample were incubated on ice for 20 min with IgM-PE isotype control (eBioscience 12-4752- 82), TRA-1-60-PE (eBioscience 12-8863-82, PE) or Tra-1-81-PE (eBioscience 12-8883-80) at 1/20 dilution. For propidium iodide (PI) staining, 100µl 1.5µM PI (Sigma) was added to 100µl cells and incubated for 10-15min on ice. Samples were pelleted and

resuspended in 150µl PBS alone (for PI stained samples) or PBS containing 50nM TOPRO3 (Invitrogen), a dead cell stain, for IgM and TRA-1-60 samples. Samples were run on the Accuri Cflow flow cytometer. Debris, TOPRO3 positive dead cells (except when deliberately analyzing dead populations) and cell doublets were excluded from the analysis.

Immunostaining.

For live PI staining, 100µl 1.5µM PI (Sigma) in PBS was added to wells containing 100µl cells/media. After 10min PI/media was aspirated and replaced with 100µl 1:10000 HOESCHT in PBS. Plates were imaged live on the Image Express Micro platform (Molecular Devices Corporation). For immunostaining, cells were fixed with 4% PFA for 20min, washed with PBS-/- and blocked with 5% NDS in 0.3% triton-X/PBS for 1 hour. Primary antibody in 1% NDS/TX/PBS was then applied for a further hour at room temperature. The antibodies used were TRA-1-60 at 1:100 (Abcam 16288, mouse), PMEL17 at 1:25 (DAKO HMB45, mouse monoclonal) or 1:500 Ki67 (Vector K451, rabbit). Wells were washed three times with 1% NDS/TX/PBS and secondary antibody, at 1:200 in 1% NDS/TX/PBS applied for 1 hour at room temperature. For TRA-1-60 Jackson anti-mouse IgM (715-485-020) was used, for PMEL17 Invitrogen Alexa Fluor 488 anti-mouse and for Ki67 Alexa Fluor 488 antirabbit was used. Wells were then washed three times with PBS-/- and 1:10,000 HOESCHT applied. These were imaged on the Image Express Micro platform (Molecular Devices Corporation); automated image analysis was performed using MetaExpress software. The best settings for this analysis were determined both by visual observation of the plates and by choosing.

The introducer tool.

The patch delivery tool was custom designed and manufactured with the aim of providing protected delivery of the therapeutic patch until its placement into the subretinal space. The device consists of a handle containing a mechanism to advance a flexible rod that passes from the wheel, through the shaft and to the tip where the rod physically pushes the patch out of the tip of the device (supplementary figure 1.). The rod is advanced by virtue of the wheel on the handle that the surgeon rolls forward to advance the patch out of the device and into position.

Clinical trial.

Subjects in the trial underwent extensive screening and follow-up investigations including (i) blood sampling for: Hematology: Hemoglobin, Hematocrit, RBC, Platelet, WBC count and differential; Chemistry: Urea, Creatinine, Glucose, Calcium, Sodium, Potassium, Chloride, Total CO_2, AST, ALT, Total Bilirubin, ALP, Uric acid, Albumin, Total protein; HIV, HepB and HepC testing; (ii) Urinalysis for pH, Glucose, Protein, Blood, Ketones, Nitrites, Leukocyte esterase, microscopy and a drug screen.

A physical examination, including head, ears, eyes, nose, mouth, skin, heart and lung, lymph nodes, gastrointestinal, musculoskeletal, and neurological systems, blood pressure, pulse rate and Electrocardiograms, was also performed.

Primary endpoints.

1. Incidence and severity of adverse events.
2. Change from baseline in Early Treatment Diabetic Retinopathy (ETDRS) best corrected visual acuity (BCVA) - Proportion of subjects with an improvement of 15 letters or more at Week 24.

Inclusion criteria.

1. Male and /or post-menopausal (defined as at least 12 consecutive months with no menses without an alternative medical cause) female subjects aged 60 years or above.
2. Diagnosis of wet age-related macular degeneration (AMD) with evidence of good foveal fixation in the study eye plus at least one of:
    - History of sudden decline in vision within 6 weeks of the time of surgery (Day 1) associated with evidence of an RPE tear extending under the fovea.
    - History of sudden decline in vision within 6 weeks of the time of surgery (Day 1) associated with a sub macular hemorrhage with greatest dimension of 6 disc diameters.
    - Evidence of failure to respond to anti-VEGF treatments as defined by declining vision ≥25 ETDRS letters within 20 weeks prior to surgery (Day 1) despite at least 3 injections of anti-VEGF.
3. BCVA value recorded of 6/36 Snellen equivalent or worse in the study eye during or within 14 d of the screening period.
4. An informed consent document signed and dated by the subject or a legal

representative.

5. Subjects who are willing and able to comply with all scheduled visits, treatment plan, laboratory tests, and other study procedures**.**

Exclusion criteria.

1. Evidence or history of clinically significant hematological, renal, endocrine, pulmonary, gastrointestinal, cardiovascular, hepatic, psychiatric, neurologic, allergic disease (including drug allergies, but excluding untreated, asymptomatic, seasonal allergies at time of dosing) or other severe acute or chronic medical or surgical condition or laboratory abnormality that may increase the risk associated with study participation or investigational product administration or may interfere with the interpretation of study results and, in the judgment of the investigator, would make the subject inappropriate for entry into this study.
2. Pregnant females; breastfeeding females; and females of childbearing potential
3. Positive urine drug screen for illicit drugs or drugs of abuse.
4. History of regular alcohol consumption exceeding 14 units/week for females or 21 units/week for males within 6 months of screening.
5. Treatment with an investigational drug within 30 d (or as determined by the local requirement, whichever is longer) or 5 half-lives preceding the first dose of study medication.
6. Blood donation of >1 pint (500 mL) within 56 d prior to dosing.
7. Subject unwilling or unable to comply with the Lifestyle Guidelines described in this protocol.
8. Contraindication to general anesthesia (as determined by the attending anesthetist).
9. Previous significant retinal disease in the study eye (other than AMD), as determined by the investigator.
10. Current or previous significant other ocular disease in the study eye, as determined by the investigator.
11. Any ocular disease in the study eye that might alter the ocular media and reduce the posterior segment view, as determined by the investigator.
12. Any previous retinal surgery in the study eye.
13. Contraindication to prednisolone, triamcinolone, cefuroxime or fluocinolone acetonide (specifically increased intra-ocular pressure or glaucoma).
14. History of sensitivity to heparin or heparin-induced thrombocytopenia.

15. Use of anti-VEGF therapy (e.g., Lucentis) within 7 d of surgery in the study eye.
16. Participation in another ongoing interventional clinical study.
17. Limited use of non-prescription medications that are not believed to affect subject safety or the overall results of the study may be permitted on a case-by-case basis following approval by the sponsor.
18. Subjects who are investigational site staff members or relatives of those site staff members or subjects who are Pfizer employees directly involved in the conduct of the study.

Visit schedule.

Subjects attended the hospital on an out-patient basis for up to three d during the screening interval (Day -21 to Day 0). Eligible subjects attended the hospital on an out-patient basis the day before surgery (Day 0) for pre-surgery assessments. Insertion of PF-05206388 (the hESC-RPE patch) occurred the following day (Day 1). Subjects were discharged from the hospital the day after surgery (Day 2). There was a second operative procedure performed at the Week 10 visit (Visit 9) whereby the silicone oil, which was inserted at the time of PF-05206388 insertion, was removed from the eye. Subjects with significant cataracts noted at screening were permitted to have the cataracts removed at the time of this second surgical procedure. For the first procedure, subjects received up to 1 mg/kg oral prednisolone (up to 60 mg maximum) daily commenced 2-4 d pre-operatively and continued for at least 2 weeks followed by a tailing off over at least 1 further week. Subjects also received single doses of sub-Tenon triamcinolone acetonide 40 mg and sub conjunctival cefuroxime (250 mg in 1 mL) after patch insertion. For the second procedure, subjects received up to 1 mg/kg oral prednisolone (up to 60 mg maximum) daily commenced 7 d pre-operatively and continued for at least 2 weeks followed by a tailing off over at least 1 further week. Subjects also received an intravitreal implant of fluocinolone acetonide either 0.19 or 0.59 mg as an anti-inflammatory agent and sub conjunctival cefuroxime (250 mg in 1 mL) post-surgery.

The first surgical procedure was carried out on Day 1, subjects were discharged from hospital on Day 2 and attended for post-surgical evaluations at Week 1, Week 2, Week 4, Week 8, Week 12, Week 16, Week 24, Week 36 and Week 52.

Surgical procedures.

Transplantation operation: patients underwent standard general anesthesia. Routine sterile povidone-iodine 5% preparation of the eye with and draping of the face was completed. The eyelids were separated with a disposable Barraquer speculum. For case 1 a cataract was removed and a single focus, one-piece, acrylic lens for emmetopria was inserted, at the time of the transplant surgery, while subject 2 was already pseudophakic. A 270 degree peritomy with a standard 23-gauge infusion and 2 further ports were inserted. Pars plana vitrectomy with induction of PVD when not present was completed with subsequent 360 degree Argon laser. A macular retinal detachment was created with a 38 gauge de Juan dual bore cannula, the retinotomy was enlarged with microscissors and the subretinal space irrigated to remove all blood and fibrin. The temporal port was widened for introduction of the delivery device and insertion of the patch into the sub retinal space. The macular was re-attached with heavy liquid and the retinotomy lasered. A routine search of the retinal periphery was completed in both cases with no iatrogenic breaks detected. Air/fluid followed by air/silicone oil exchange was carried out. The ports were sutured and the infusion removed. Sub-Tenon triamcinolone acetonide 40mg and subconjunctival cefuroxime (250 mg/1 ml) were injected followed by sub-Tenon (0.5% bupivacaine).

Removal of Silicone Oil: silicone oil was removed under sub-Tenon local anaesthesia. A 23-gauge infusion was inserted in the infero-temporal quadrant and a second port created to aspirate the oil. The retinal periphery was examined for breaks. The ports were closed and subconjunctival antibiotics were given. For subject 2 an operation to reattach a detached retina, consisting of epiretinal membrane peeling, inferior 180 degree retinectomy and laser, was carried out before the oil removal.

Ocular tests and examinations.

Biomicroscopic evaluation and intra-ocular pressure measurement were carried out using a Haag-Streit 900 slit-lamp (Koeniz, Switzerland) and Goldmann applanation tonometer.

Fundus photography, angiography.

Colour, red-free fundus photographs and standard fluorescein and indocyanine green angiography (50°) were acquired through dilated pupils using the Topcon TRC Retinal Camera (Oakland, NJ, USA).

Spectral-domain OCT scan and cSLO reflectance imaging.

Volume scan and EDI volume scan, 20°x20°, 49 sections, ART 12, High Speed scans and 30°, 55° short-wave reflectance autofluorescence images were acquired through dilated pupils using the Spectralis OCT (Heidelberg Engineering GmbH, Heidelberg, Germany)

Adaptive optics.

AO images were acquired through dilated pupils using the ImagineEyes Camera (Orsey, France). Alignment and data collection was repeated for several retinal locations.
For calculation of cellular density, a freely available image-processing program (ImageJ, National Institutes of Health, Bethesda, Maryland) was used to manually identify the cones in each subject's retinal image.

Pattern ERG, full-field ERG and EOG.

Pattern ERG, full-field ERG and EOG were performed according the ISCEV standards. Dark-adapted ERGs were recorded to flashes of 0.01 and 10.0 cd.s.m-2 (DA0.01; DA10.0); light adapted responses were recorded to flashes of 3.0 cd.s.m-2 (30Hz and 2Hz).

Automated perimetry.

Visual fields were assessed using Humphrey Field Analyzer (Carl Zeiss Meditec, AG, Jena, Germany). Central 24-2 Threshold tests were performed using Goldmann III white stimulus at background luminance of 31.5ASB, in SITA-FAST strategy.

Microperimetry.

A customized rectangular grid of 9-23 loci covering the area of the RPE patch was used in Nidek MP1 Microperimeter (NAVIS software 1.7.2, Nidec Technologies, Padova, Italy). Stimuli were set to Goldmann III-V size, white color, 200ms duration and 0-20dB intensity with background luminance at 1.27cd/m^2. A single red-cross 2-3° target was used for 30 seconds fixation stability assessment. A 4-2 staircase strategy was employed to assess the retinal sensitivity through dilated pupils after 15min dark adaptation.

ETDRS/logmar best corrected visual acuity (BCVA) - distant and near, including contrast sensitivity (CS).

Refracted BCVA was tested by Independent Trained optometrists using the Early

Treatment of Diabetic Retinopathy Study (ETDRS) charts and CS the Pelli-Robson chart at 1 meter.

Minnesota reading test (MNREAD).

The MNREAD sentences were used to assess the visual processing capabilities and eye-movement control required for normal text reading. Each sentence contains 60 characters (including a space between each word and at the end of each line) printed as three lines with even left and right margins. The vocabulary used in the sentences is selected from high-frequency words that appear in second- and third-grade reading material. The charts contain sentences with 19 different print sizes. From the recommended viewing distance of 40 cm (16 in.) the print size ranges from +1.3 to -0.5 logMAR (Snellen equivalents: 20/400-20/6).

B-mode orbital ultrasound.

Ultrasound scans were acquired through sterile gel, using the ACUSON Sequoia^{TM}512 system (Siemens Healthcare, USA)

Ocular oncologist review.

Specialist Ocular oncologists reviewed the patients with biomicroscopic evaluation and review of images from the ultrasound, fundus photography and fundus angiography.

Data validation.

This manuscript is generated from an unlocked database and includes some data that Pfizer is not responsible for validating/storing.

Data availability statement.

The majority of data generated or analysed during this study are included in this published article and its supplementary information. Any further data concerning the current study are available from the corresponding author on reasonable request. There are no accession codes, unique identifiers, or web links to publicly available datasets related to this study.

Online Methods References

35. Hewitt, Z. A., K. J. Amps, and H. D. Moore. 2007. 'Derivation of GMP raw materials for use in regenerative medicine: hESC-based therapies, progress toward clinical application', *Clin Pharmacol Ther*, **82**: 448-52.

36. Carr, A. J. et al. Molecular characterization and functional analysis of phagocytosis by human embryonic stem cell-derived RPE cells using a novel human retinal assay. *Mol Vis* **15**:283-295 (2009).

37. Mao, Y. & Finnemann, S. C. Analysis of photoreceptor outer segment phagocytosis by RPE cells in culture. *Methods Mol. Biol.* **935**, 285–295 (2013).

38. Ramsden, C. M., et al. (2017). Rescue of the MERTK phagocytic defect in a human iPSC disease model using translational read-through inducing drugs. *Sci Rep.* **7**(1): 51.

Shef 1.3 expansion	Shef 1.3 differentiation	Shef1.3-derived RPE isolation and expansion		Shef1.3-derived RPE as an ATMP
VTN-N coating	Plasma derived vitronectin	CELLstart	Plasma derived vitronectin	Plasma derived vitronectin
T25 flasks until confluent	*T25 flasks upto 22 weeks*	*48-well plates 5 -16 weeks*	*Transwell inserts 3 - 20 weeks*	*PET membrane 8 hours*
Essential 8 medium	**TLP medium**			**Saline**
• Appearance and viability • Karyotype	• Appearance and viability • Sterility and mycoplasma	• Appearance and viability • Sterility • Cell count	• Appearance and viability • Mycoplasma • Lin28 ISH (impurity) • PMEL17 ICC (purity)	• VIR test • Sterility, endotoxin and mycoplasma

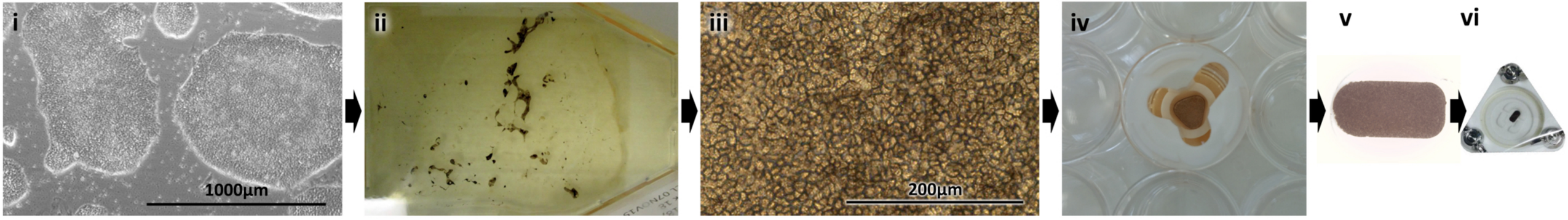

a

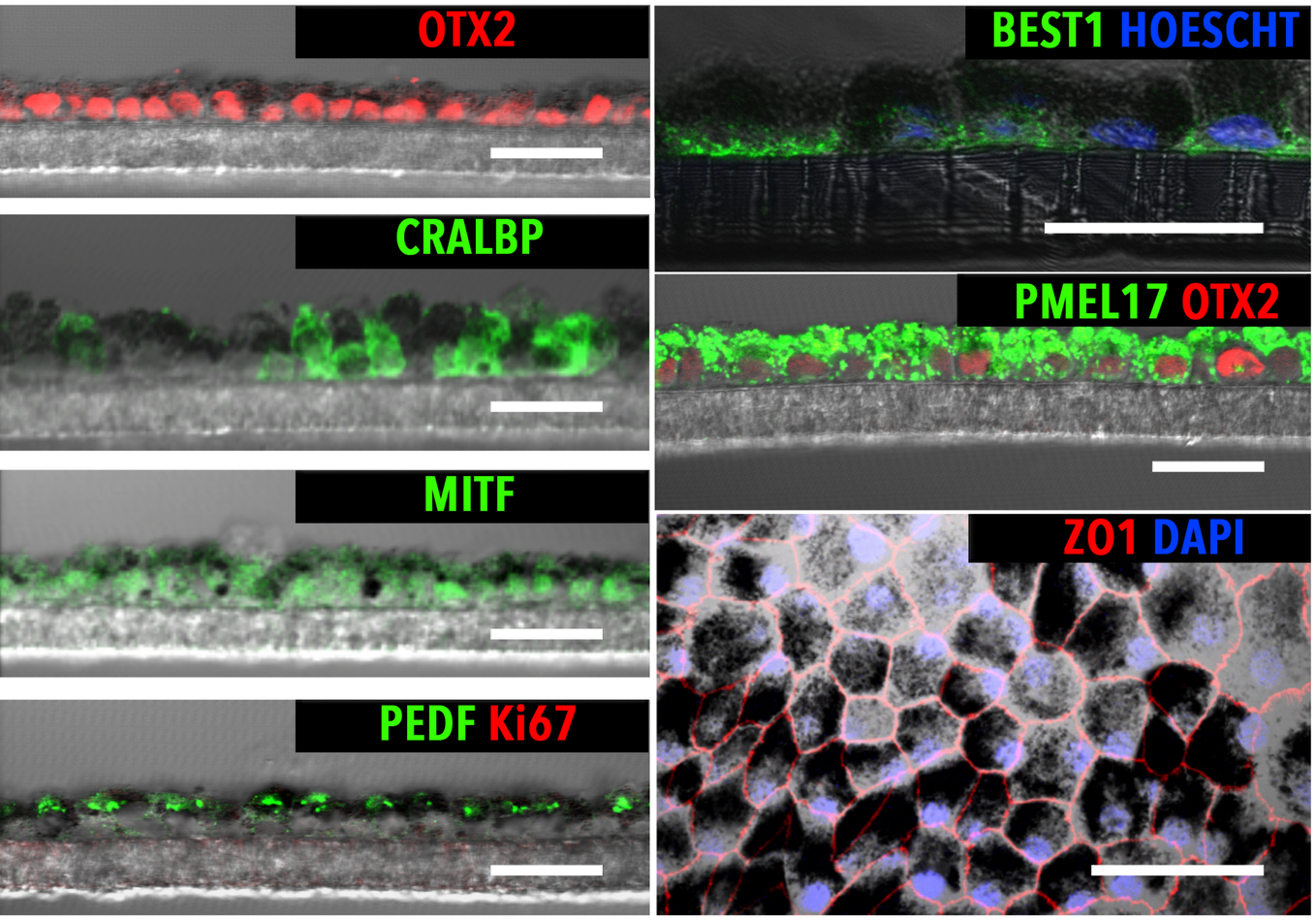
OTX2
BEST1 HOESCHT
CRALBP
PMEL17 OTX2
MITF
ZO1 DAPI
PEDF Ki67

b

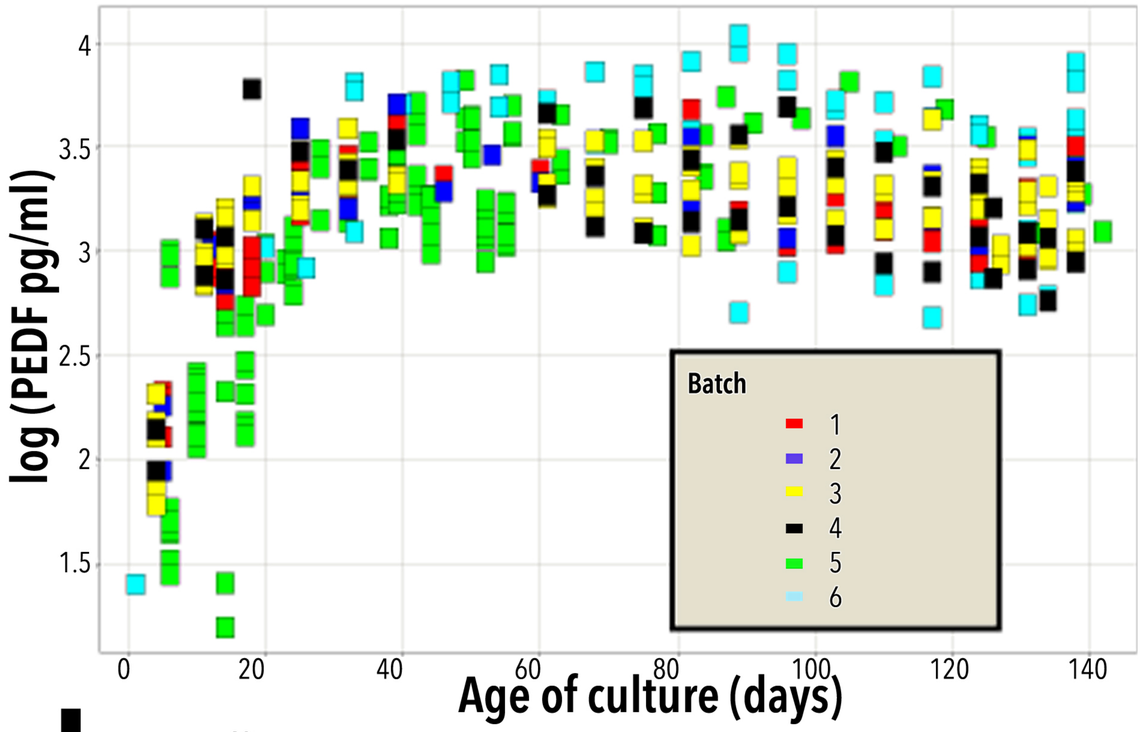
log (PEDF pg/ml)
Age of culture (days)
Batch
1
2
3
4
5
6

c

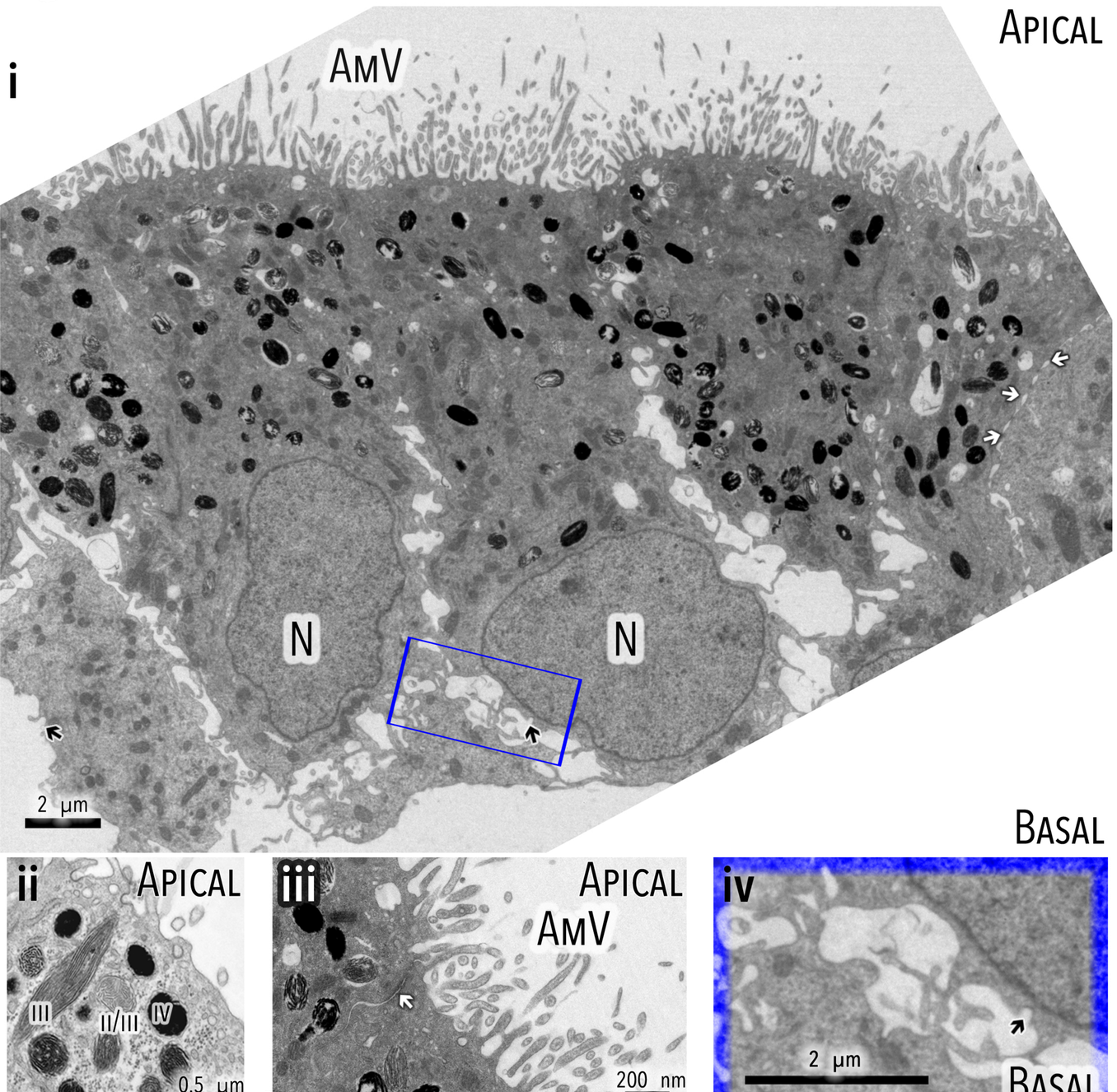
i
Apical
AMV
N
N
2 µm
Basal
ii
Apical
III
II/III
IV
0.5 µm
iii
Apical
AMV
200 nm
iv
2 µm
Basal

d

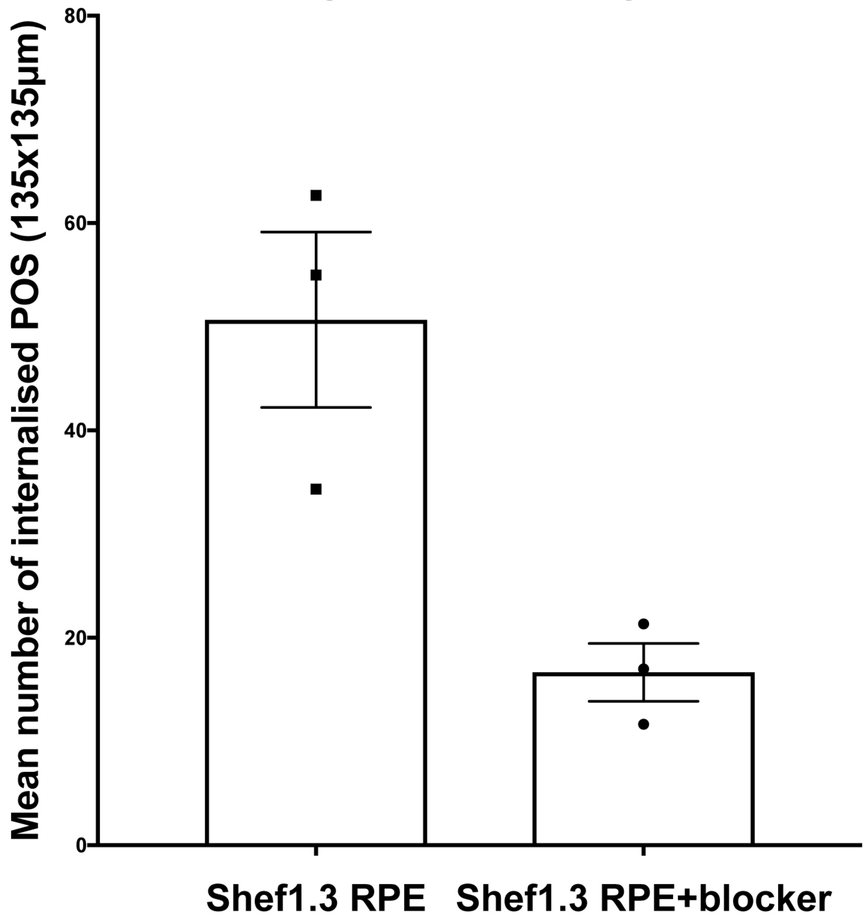
Mean number of internalised POS (135x135µm)
Shef1.3 RPE
Shef1.3 RPE+blocker

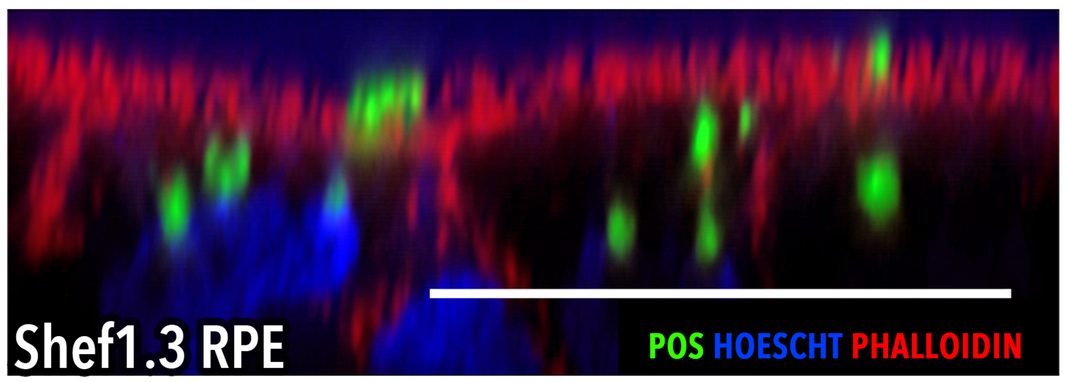
Shef1.3 RPE
POS HOESCHT PHALLOIDIN

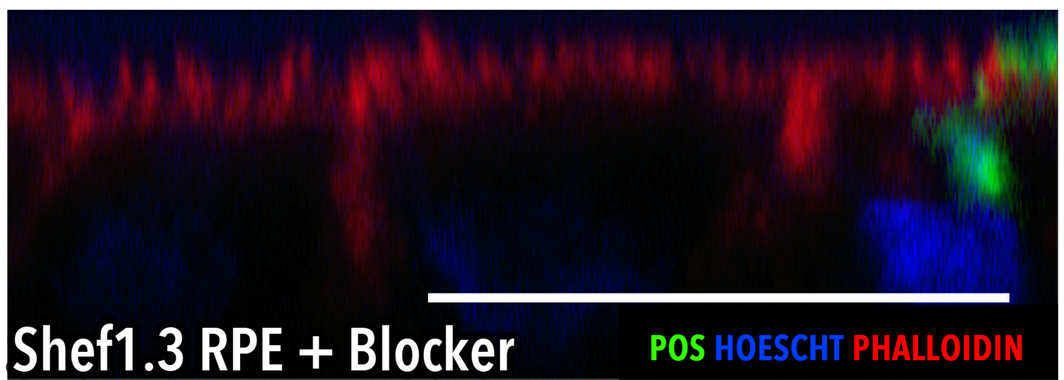
Shef1.3 RPE + Blocker
POS HOESCHT PHALLOIDIN

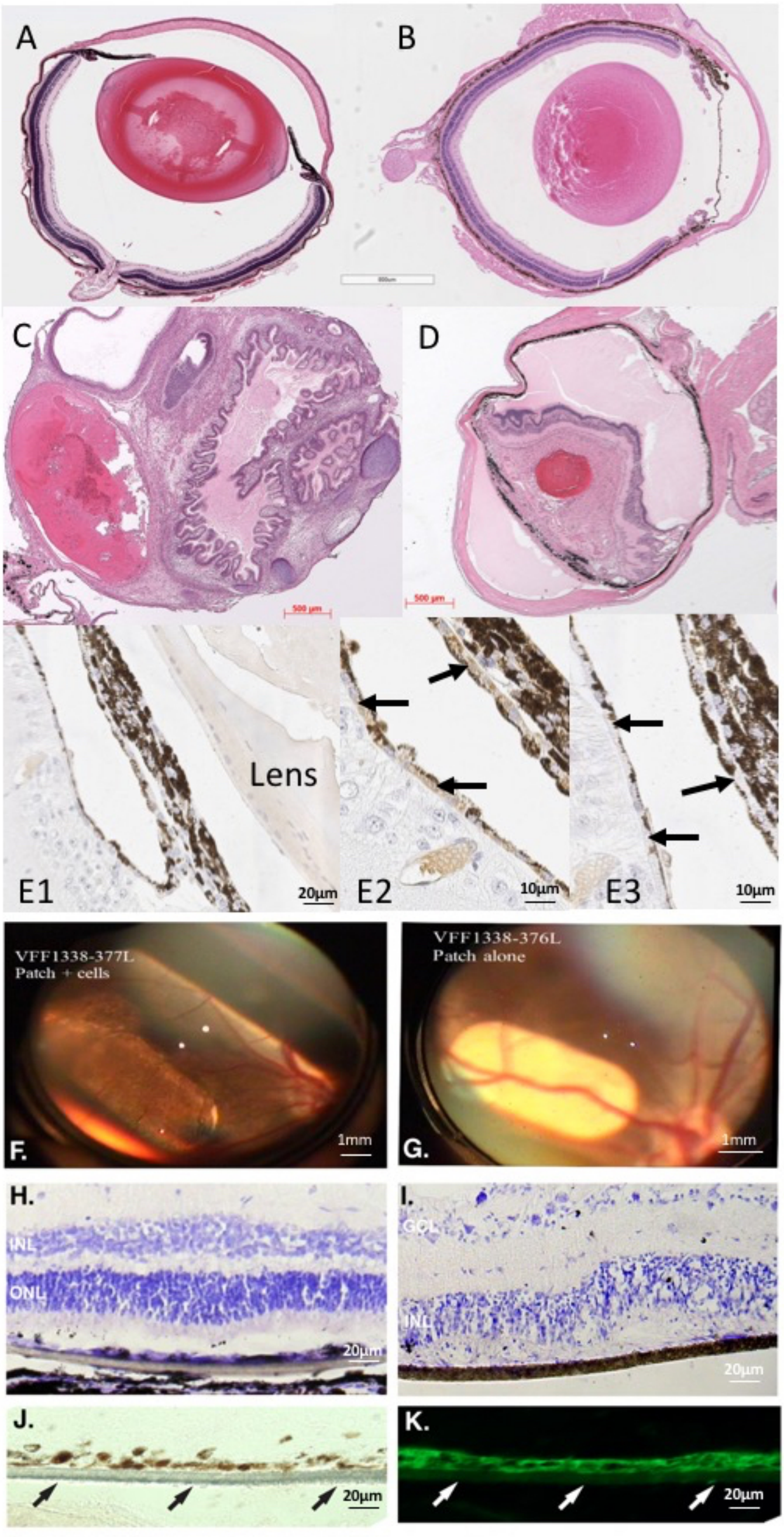
A
B
C
D
500 µm
500 µm
Lens
E1
20µm
E2
10µm
E3
10µm
VFF1338-377L
Patch + cells
F.
1mm
VFF1338-376L
Patch alone
G.
1mm
H.
INL
ONL
20µm
I.
GCL
INL
20µm
J.
20µm
K.
20µm

a1

b1

*

16

x

12

y

0

0

0

18

20

20

16

x

12

§

y

a2

27 / 49

200 µm

b2

27 / 49

200 µm

c1

x

c2

y

520 µm

x

520 µm

y

d1

x

d2

e1

x

y

e2

x

y

e3

x

y

a1

b1

*

§

a2

b2

c1

x

520 µm

c2

y

520 µm

d1

x

d2

e1

x

y

e2

x

y

e3

x

y

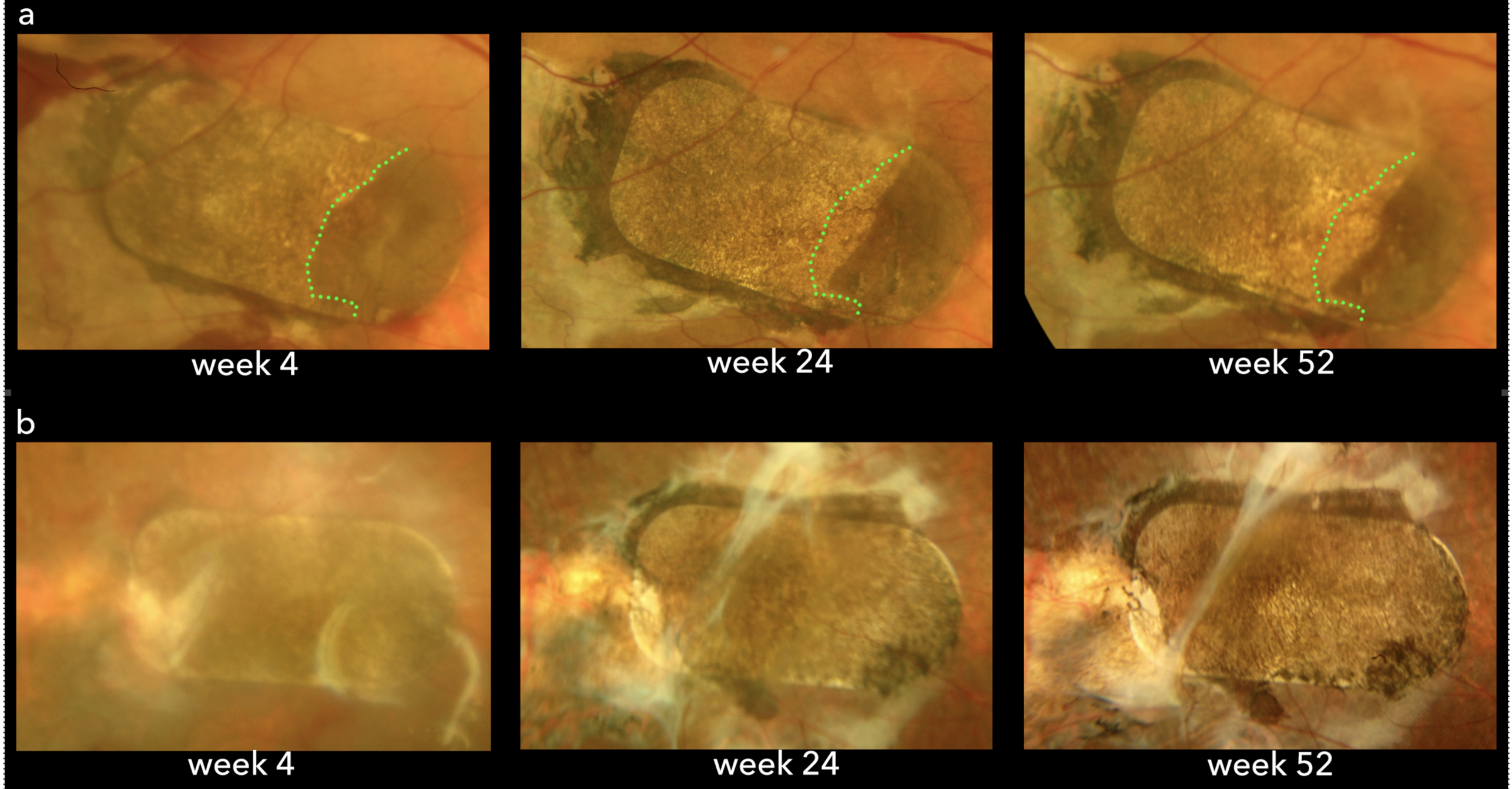
a
week 4
week 24
week 52
b
week 4
week 24
week 52

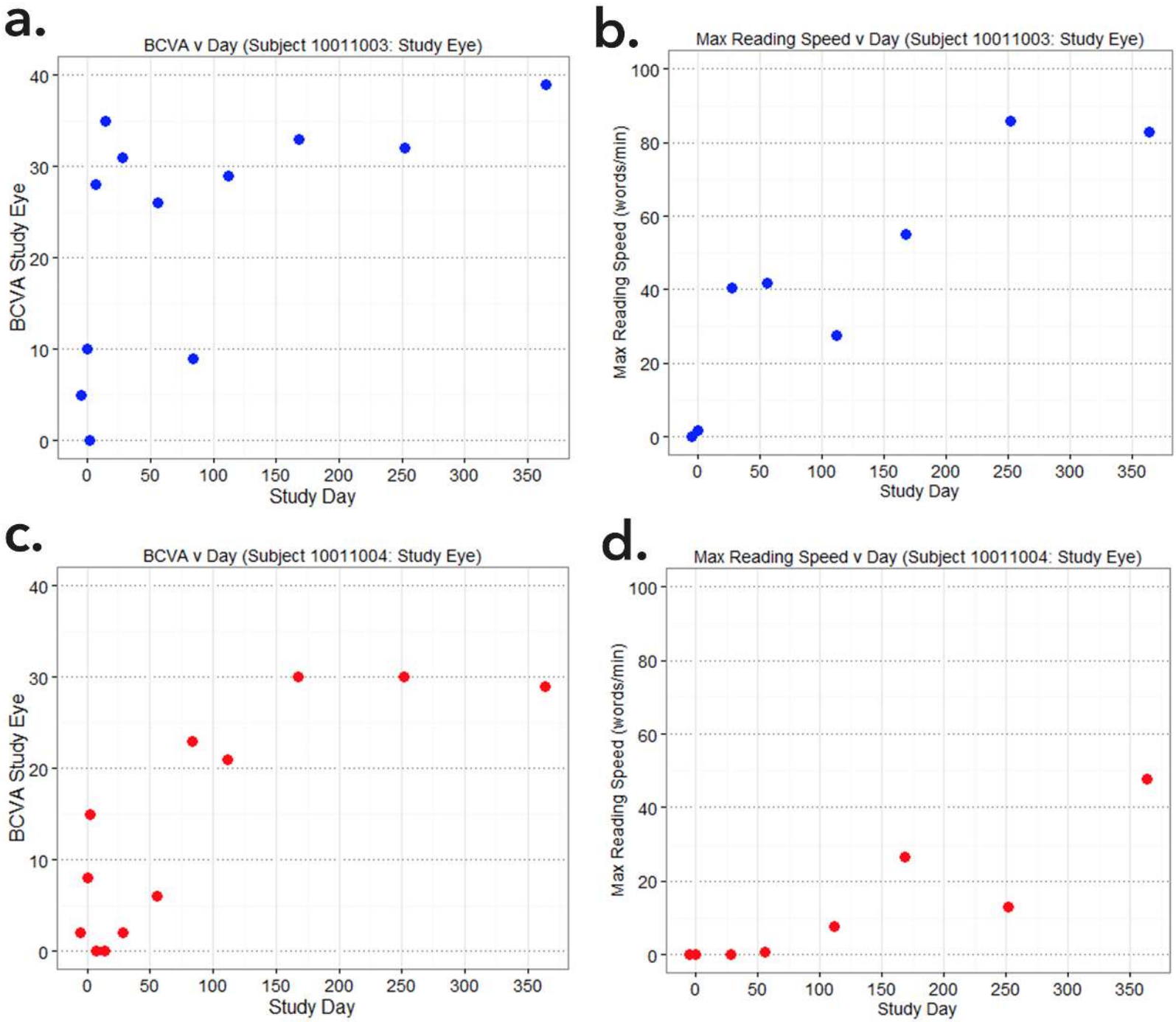
a.
BCVA v Day (Subject 10011003: Study Eye)
BCVA Study Eye
Study Day
b.
Max Reading Speed v Day (Subject 10011003: Study Eye)
Max Reading Speed (words/min)
Study Day
c.
BCVA v Day (Subject 10011004: Study Eye)
BCVA Study Eye
Study Day
d.
Max Reading Speed v Day (Subject 10011004: Study Eye)
Max Reading Speed (words/min)
Study Day